Supporting Information for

A Comparative Study of Redox-Active Dithiafulvenyl-Functionalized 1,3,6,8-Tetraphenylpyrene Derivatives

*Farshid Shahrokhi, Maryam F. Abdollahi, and Yuming Zhao**

Department of Chemistry, Memorial University of Newfoundland
St. John's, NL, Canada A1B 3X7
*Email: yuming@mun.ca

Table of Content

1. NMR Spectra of Compounds 5, and 7-9

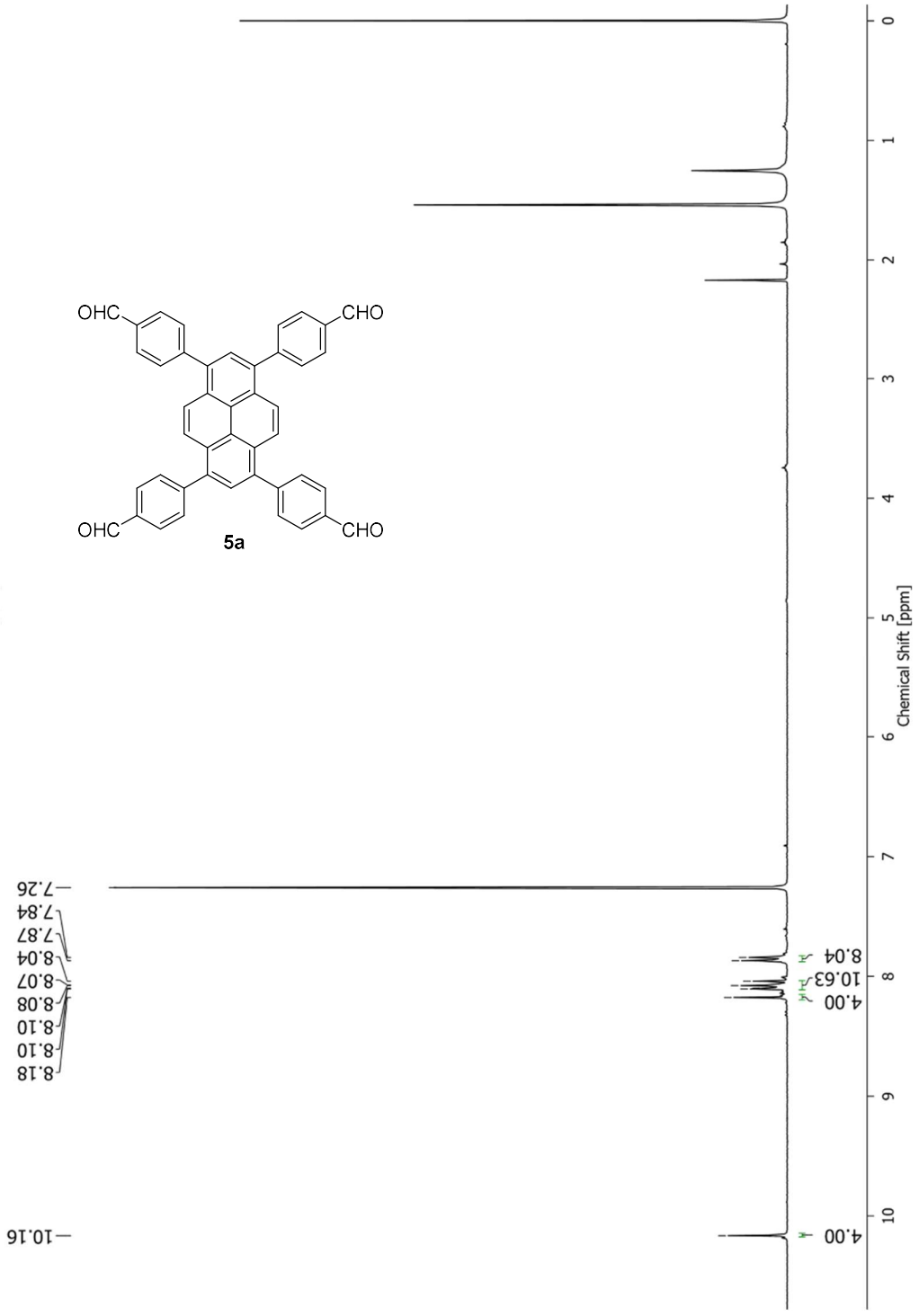

Fig. S-01 ^{1}H NMR (300 MHz, $CDCl_3$) of compound **5a**.

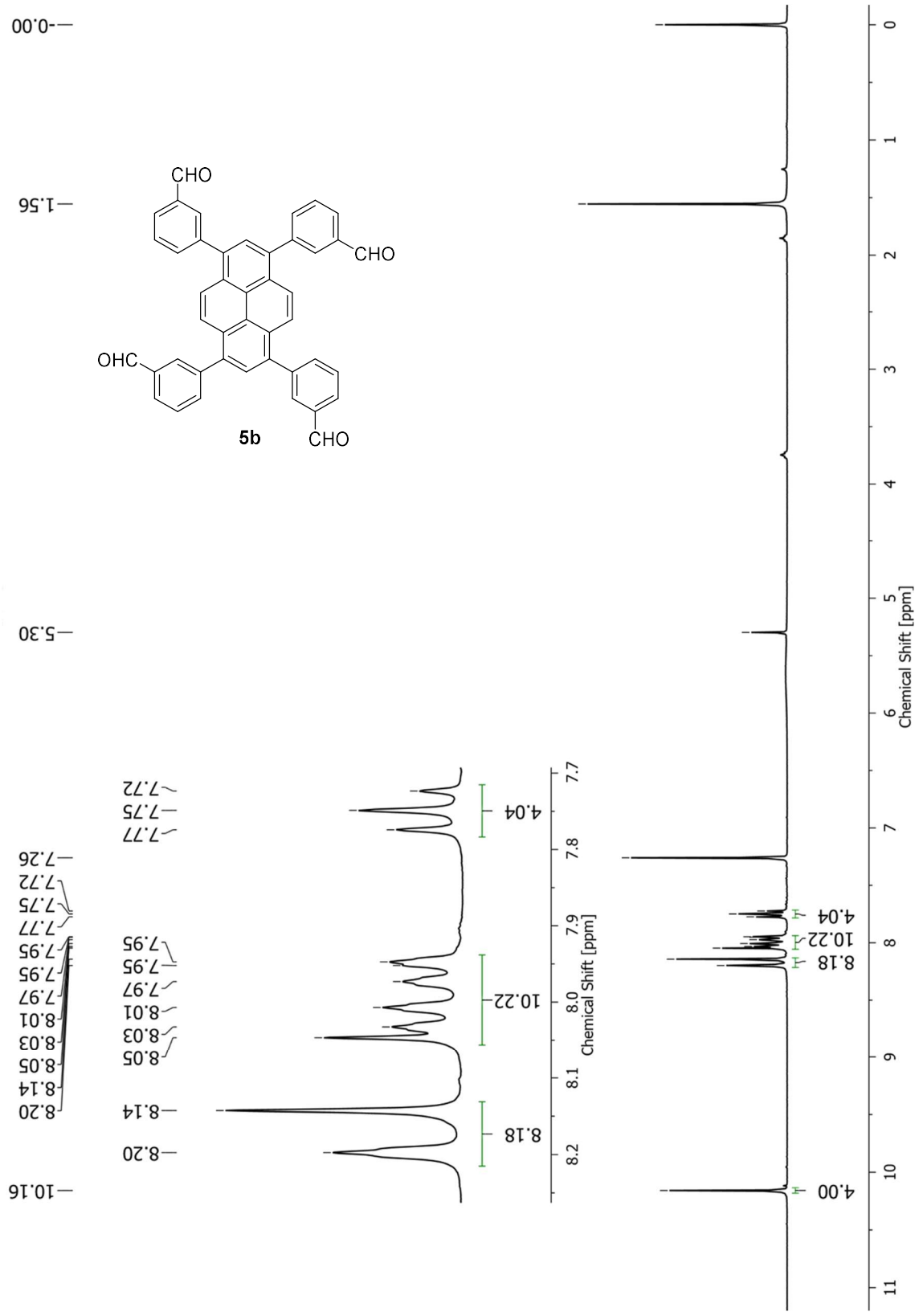

Fig. S-02 ^{1}H NMR (300 MHz, $CDCl_3$) of compound **5b**.

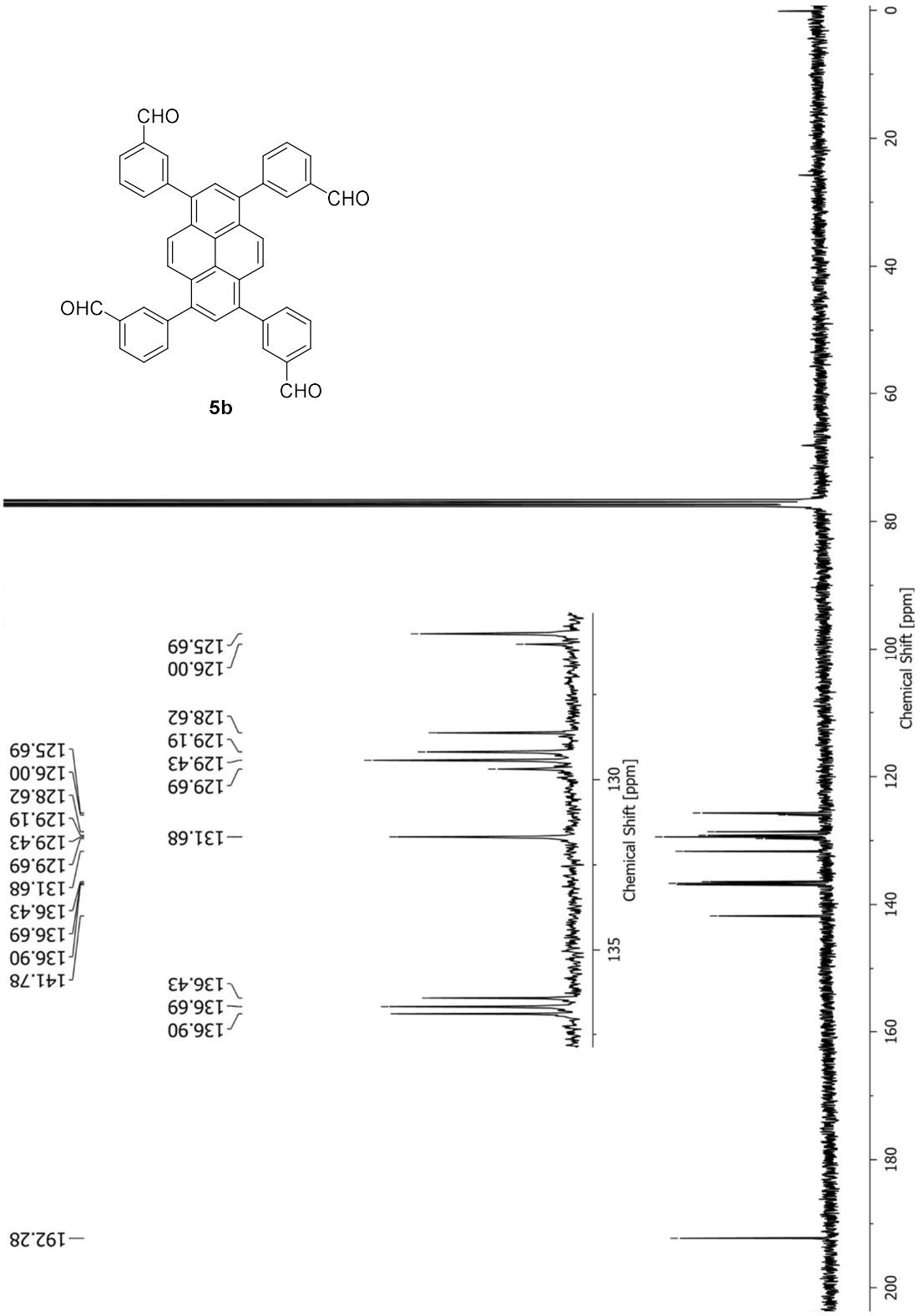

Fig. S-03 $^{13}C\{^{1}H\}$ NMR (75 MHz, $CDCl_3$) of compound **5b**.

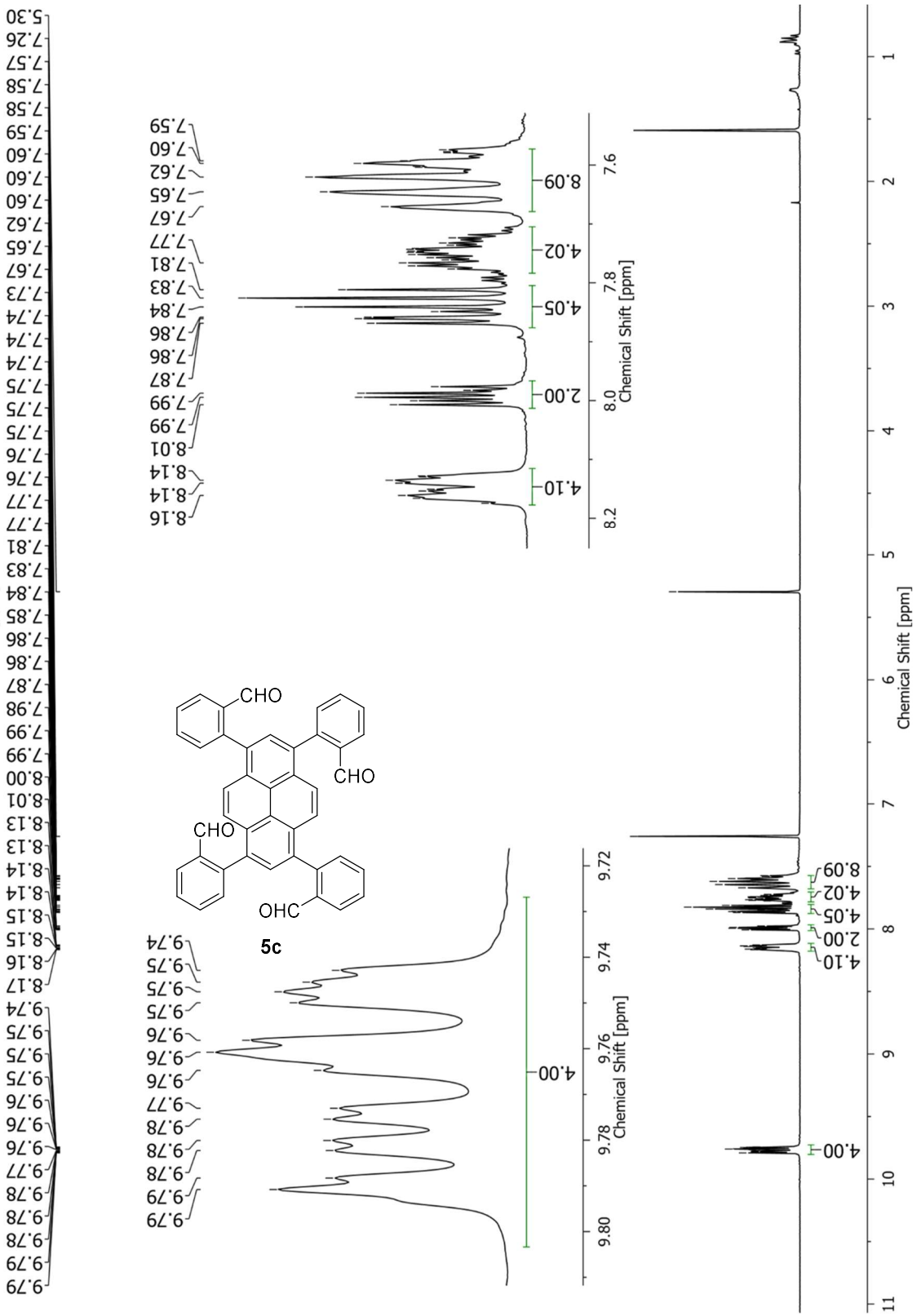

Fig. S-04 ^{1}H NMR (300 MHz, $CDCl_3$) of compound **5c**.

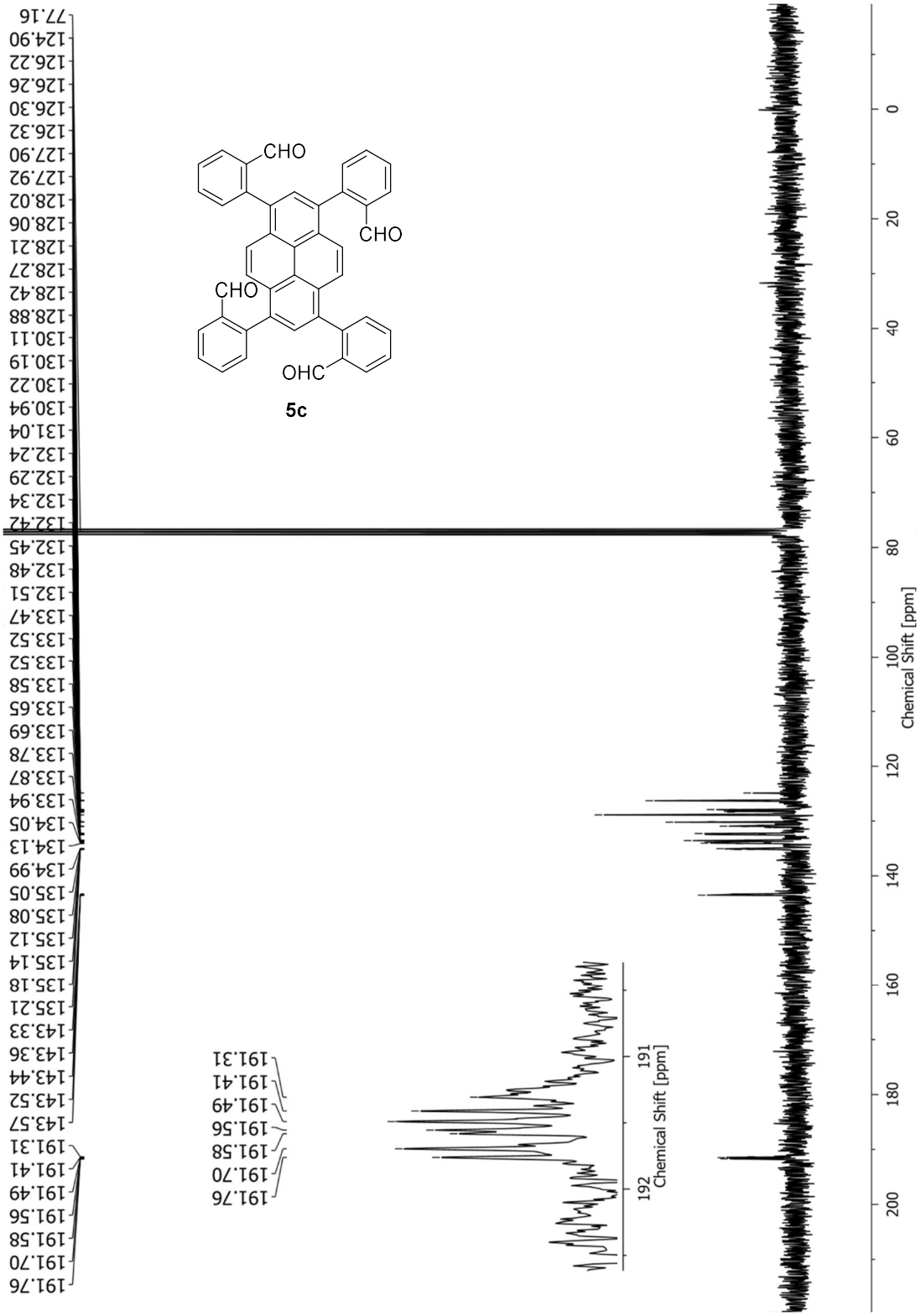

Fig. S-05 $^{13}C\{^{1}H\}$ NMR (75 MHz, $CDCl_3$) of compound **5c**.

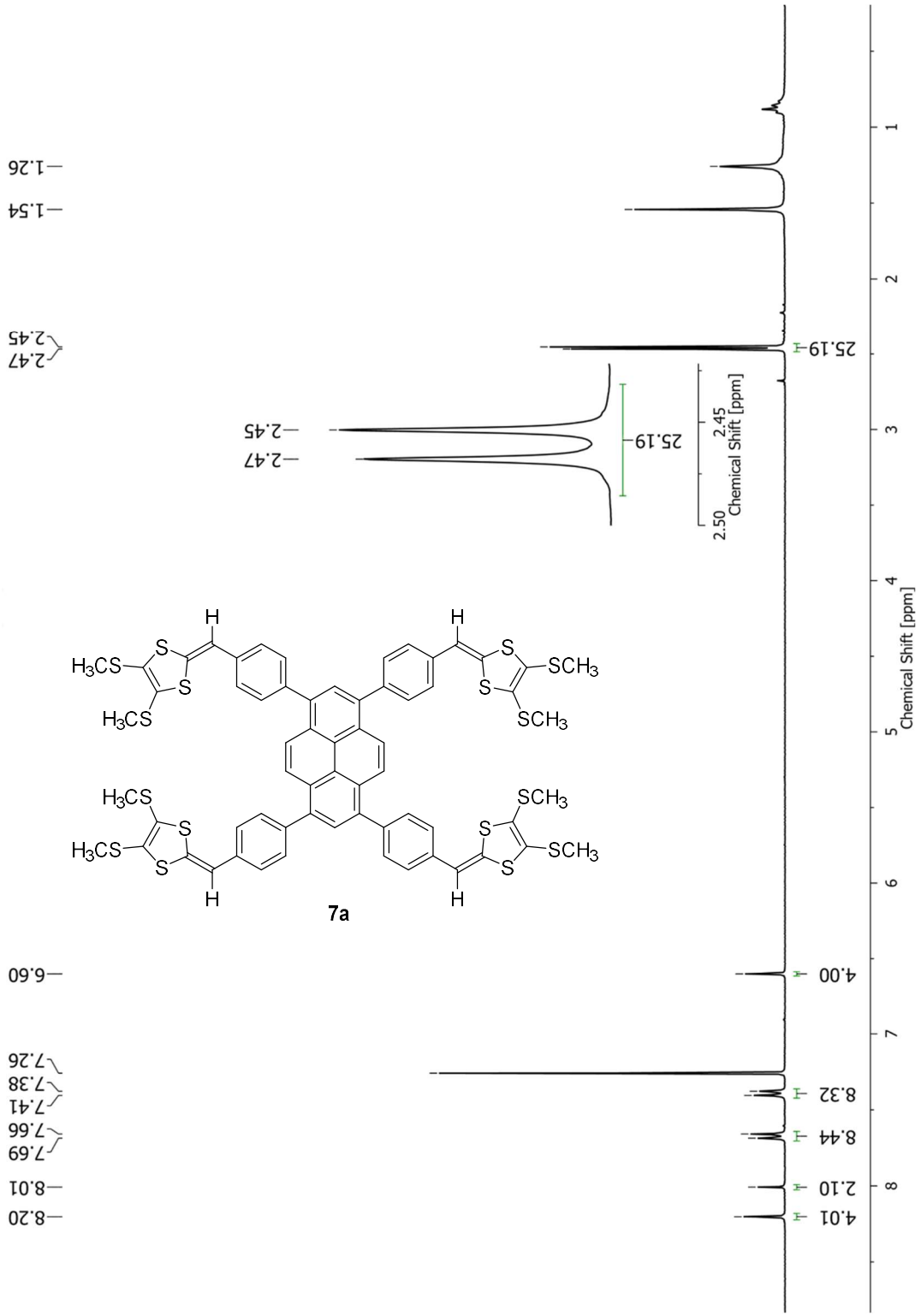

Fig. S-06 ^{1}H NMR (300 MHz, $CDCl_3$) of compound **7a**.

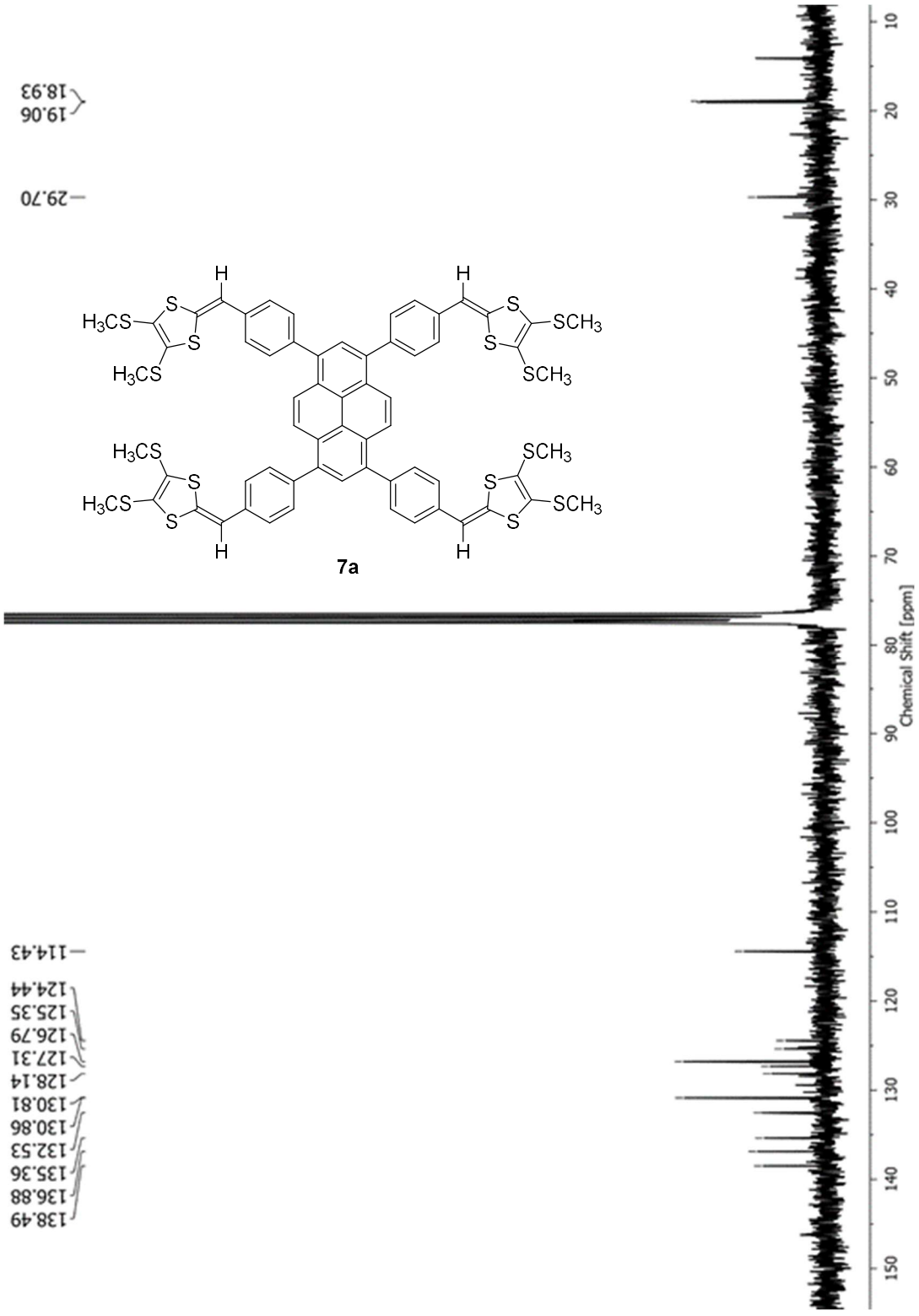

Fig. S-07 $^{13}C\{^{1}H\}$ NMR (75 MHz, $CDCl_3$) of compound **7a**.

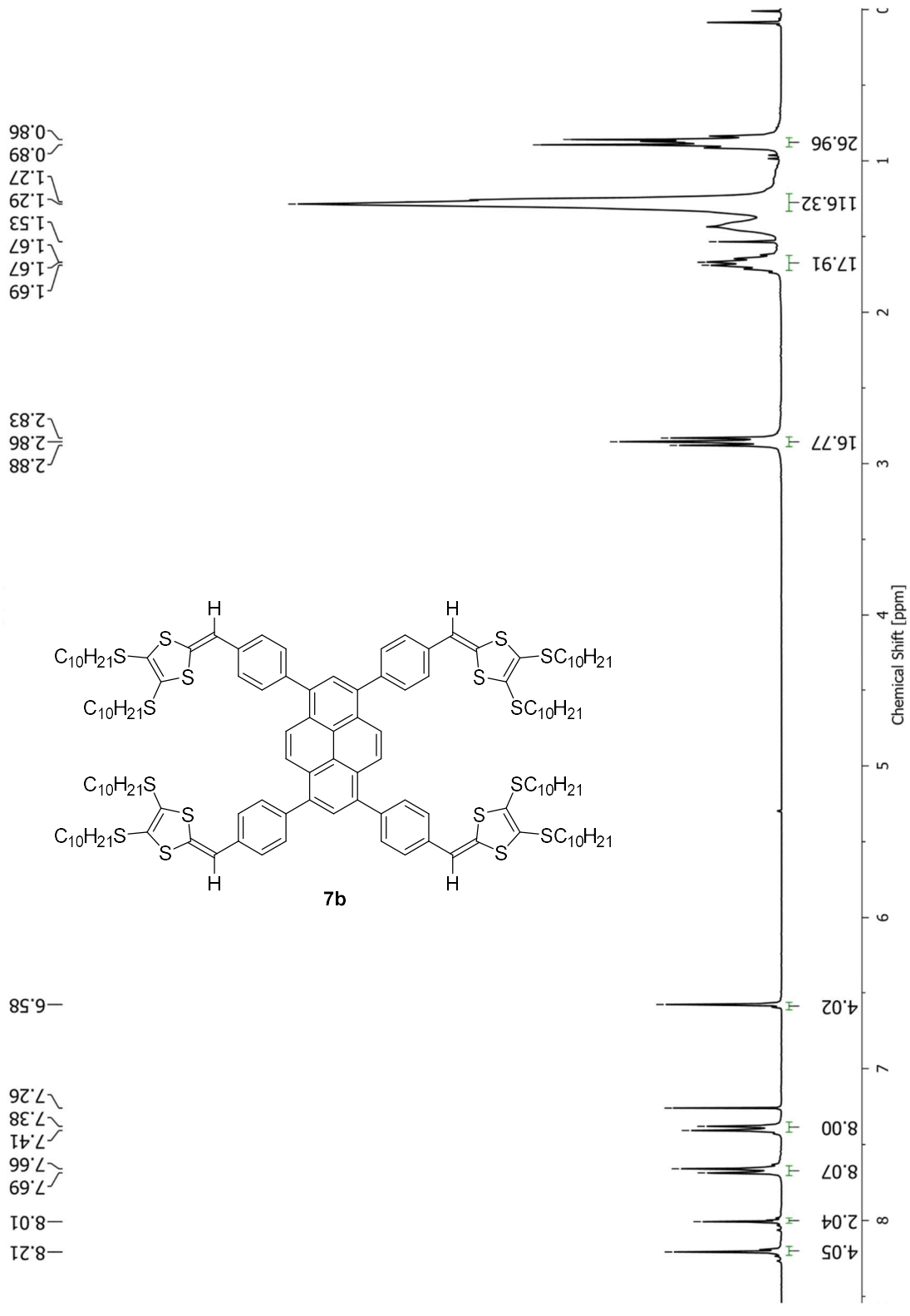

Fig. S-08 ^{1}H NMR (300 MHz, $CDCl_3$) of compound **7b**.

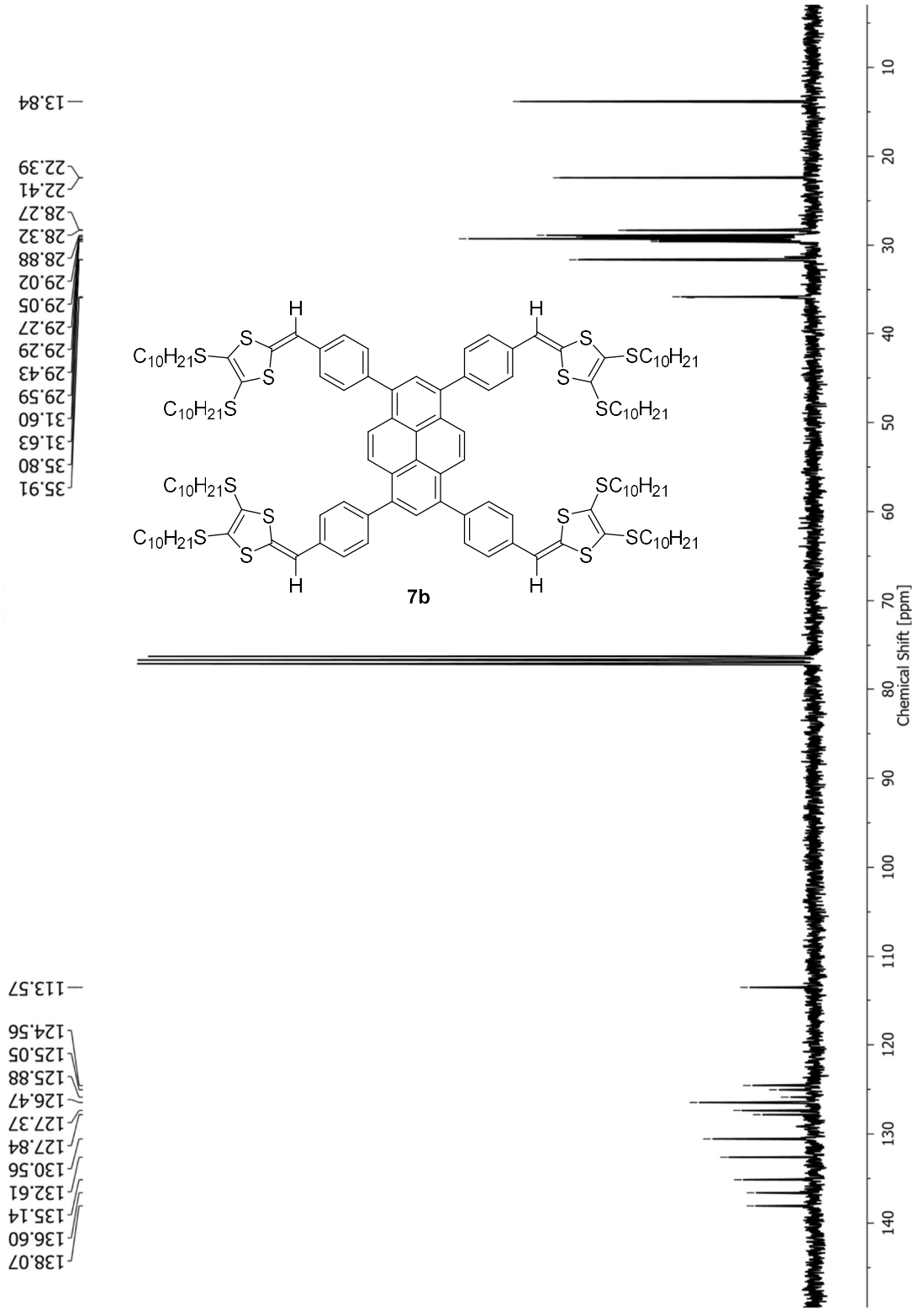

Fig. S-09 $^{13}C\{^{1}H\}$ NMR (75 MHz, $CDCl_3$) of compound **7b**.

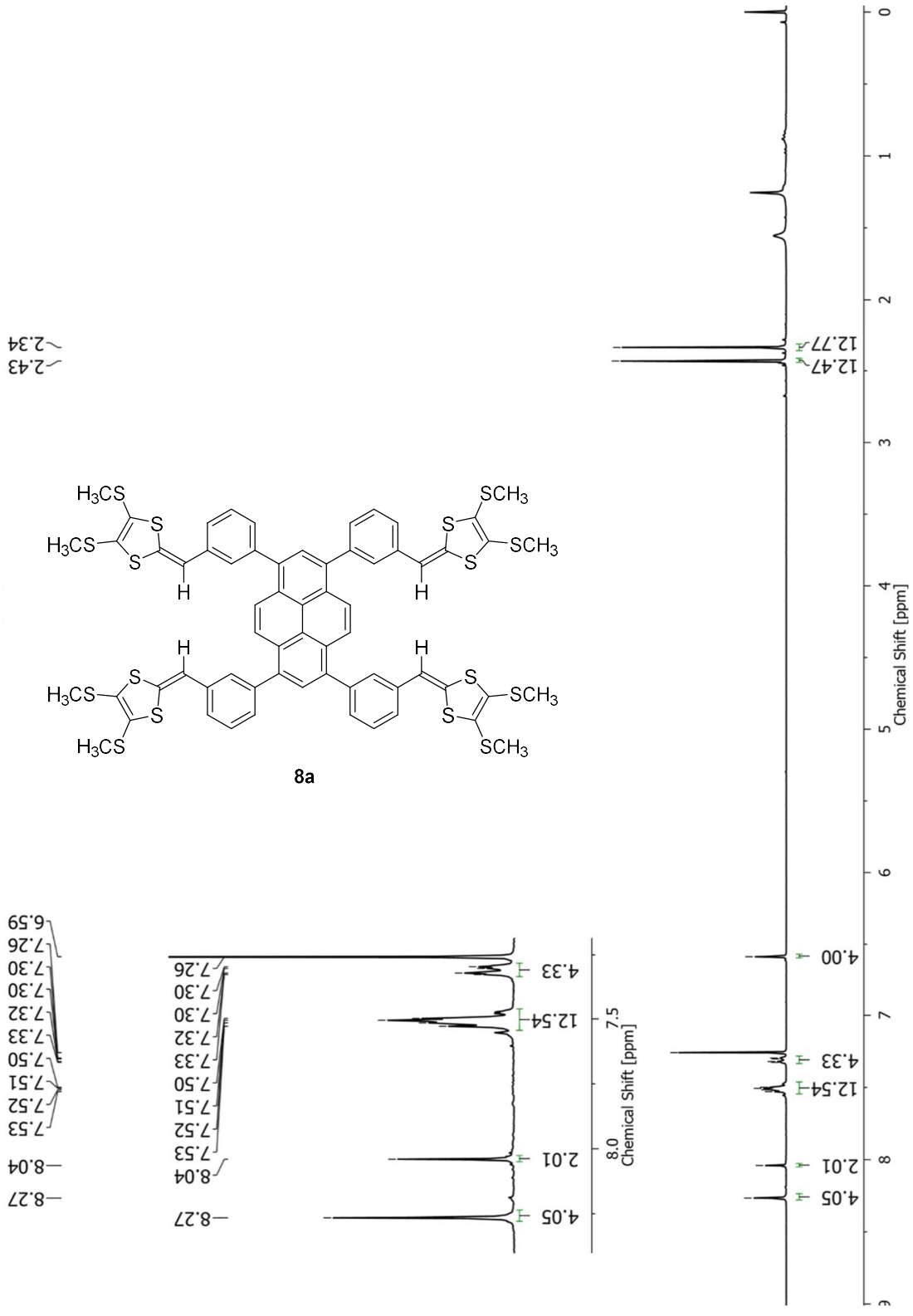

Fig. S-10 ^{1}H NMR (300 MHz, $CDCl_3$) of compound **8a**.

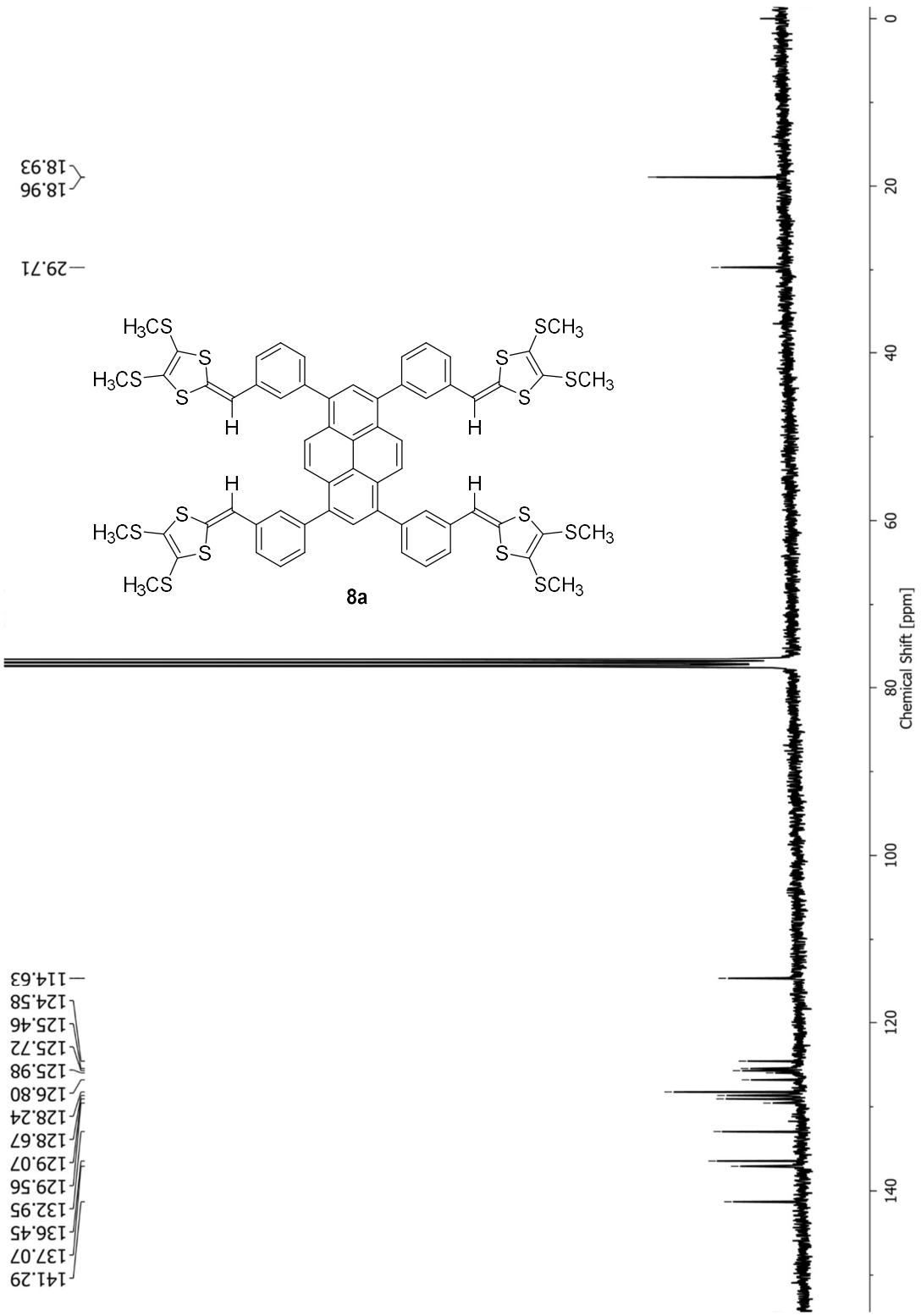

Fig. S-11 $^{13}C\{^{1}H\}$ NMR (75 MHz, $CDCl_3$) of compound **8a**.

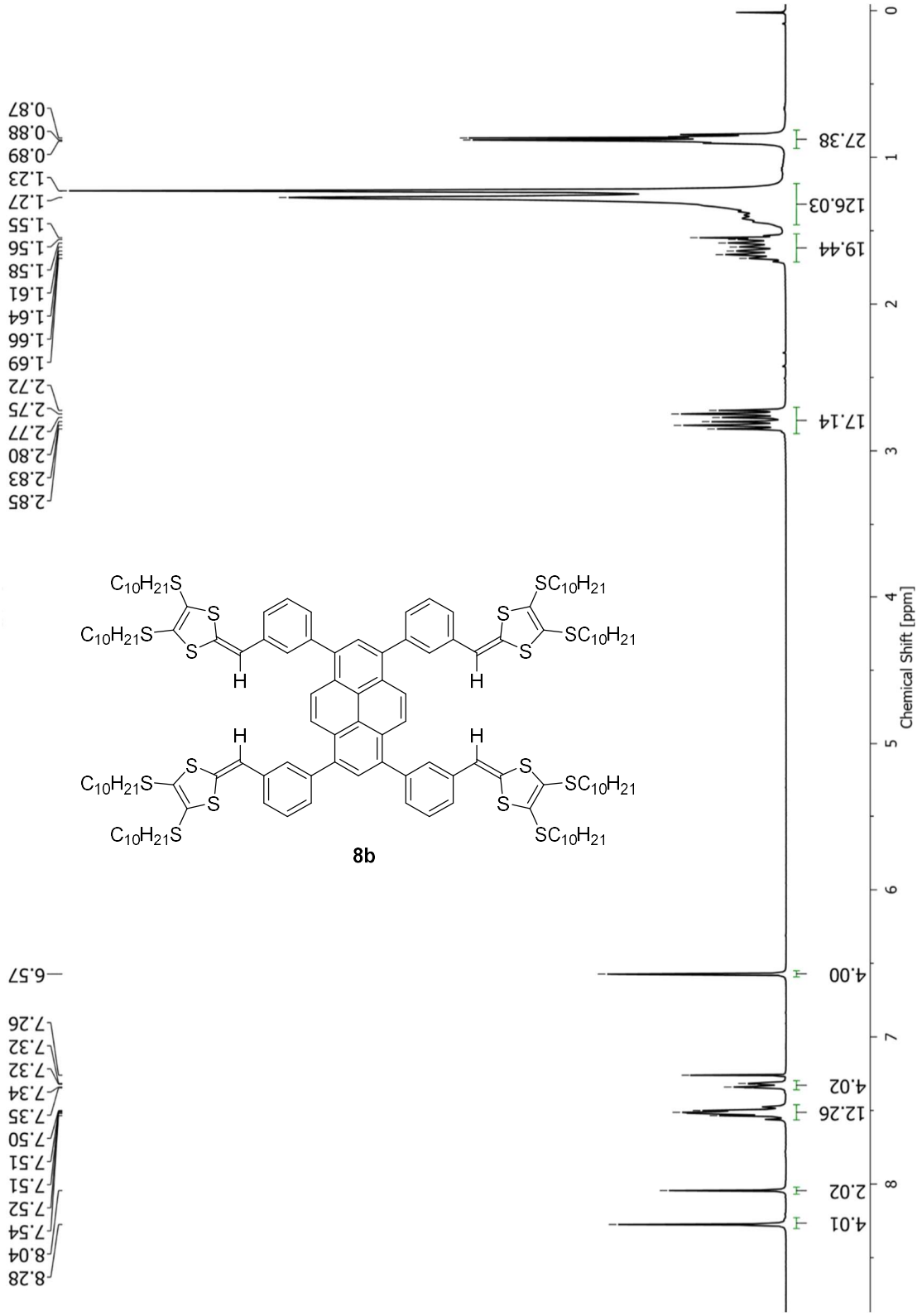

Fig. S-12 ^{1}H NMR (300 MHz, $CDCl_3$) of compound **8b**.

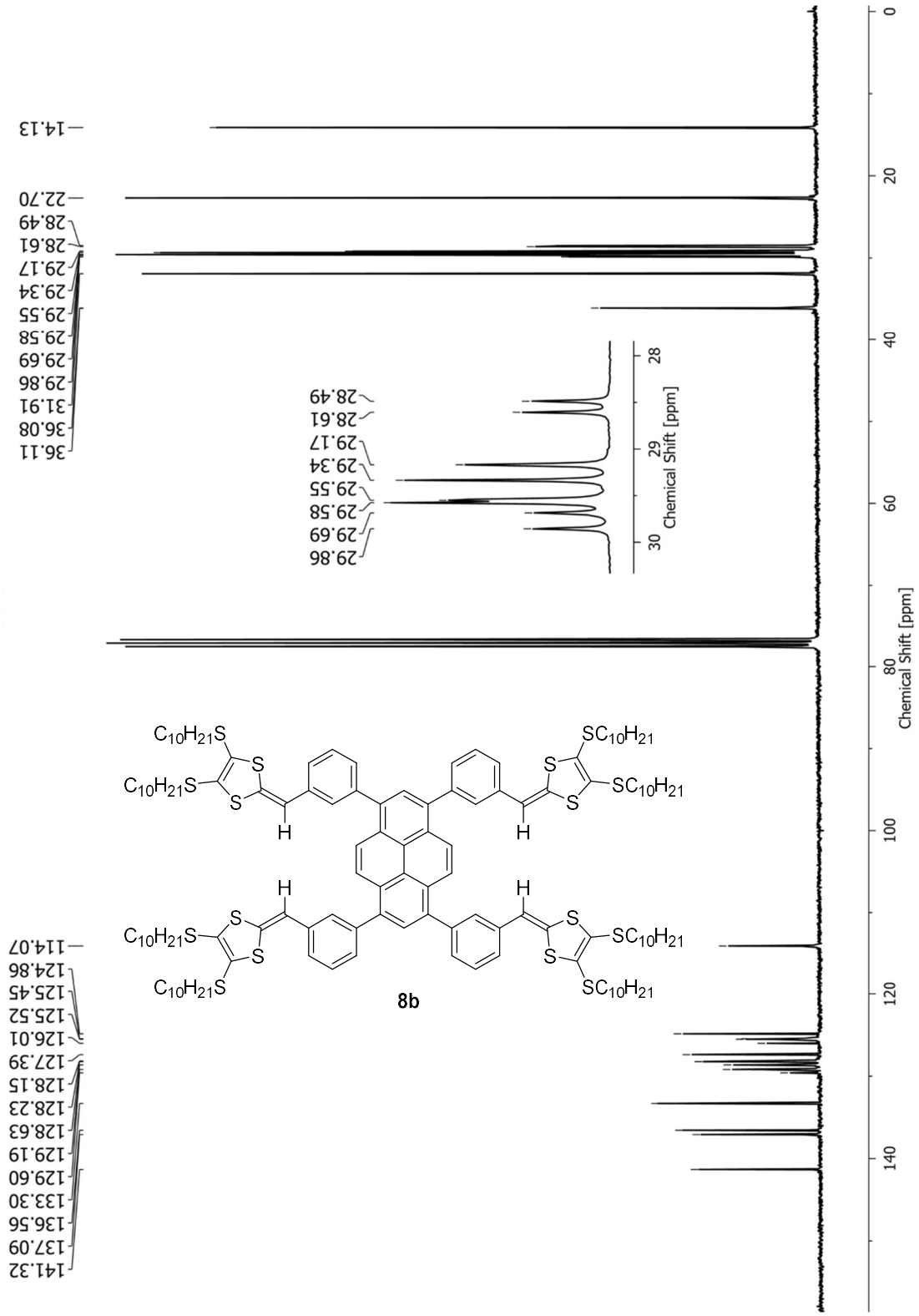

Fig. S-13 $^{13}C\{^{1}H\}$ NMR (75 MHz, $CDCl_3$) of compound **8b**.

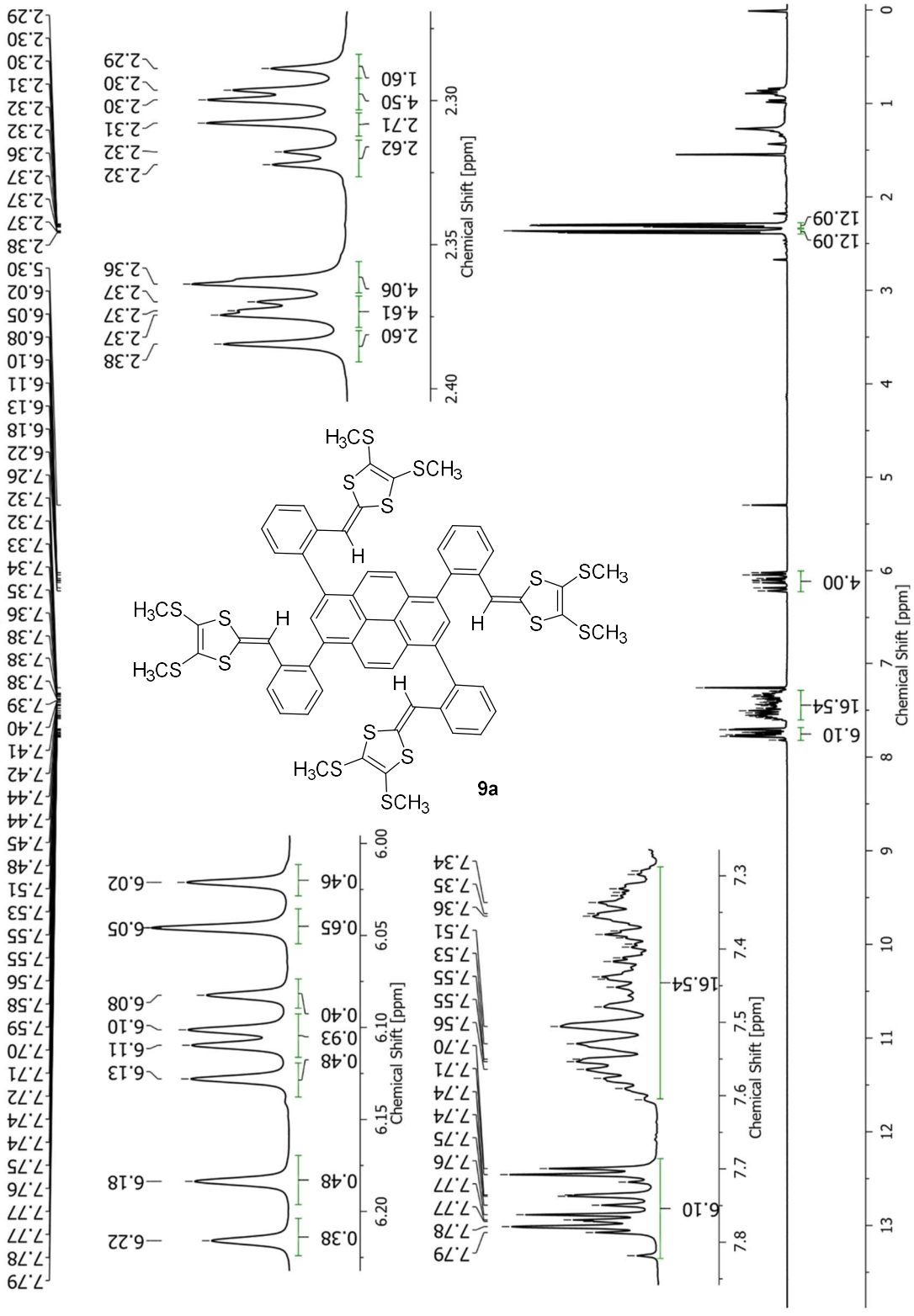

Fig. S-14 ^{1}H NMR (300 MHz, $CDCl_3$) of compound **9a**.

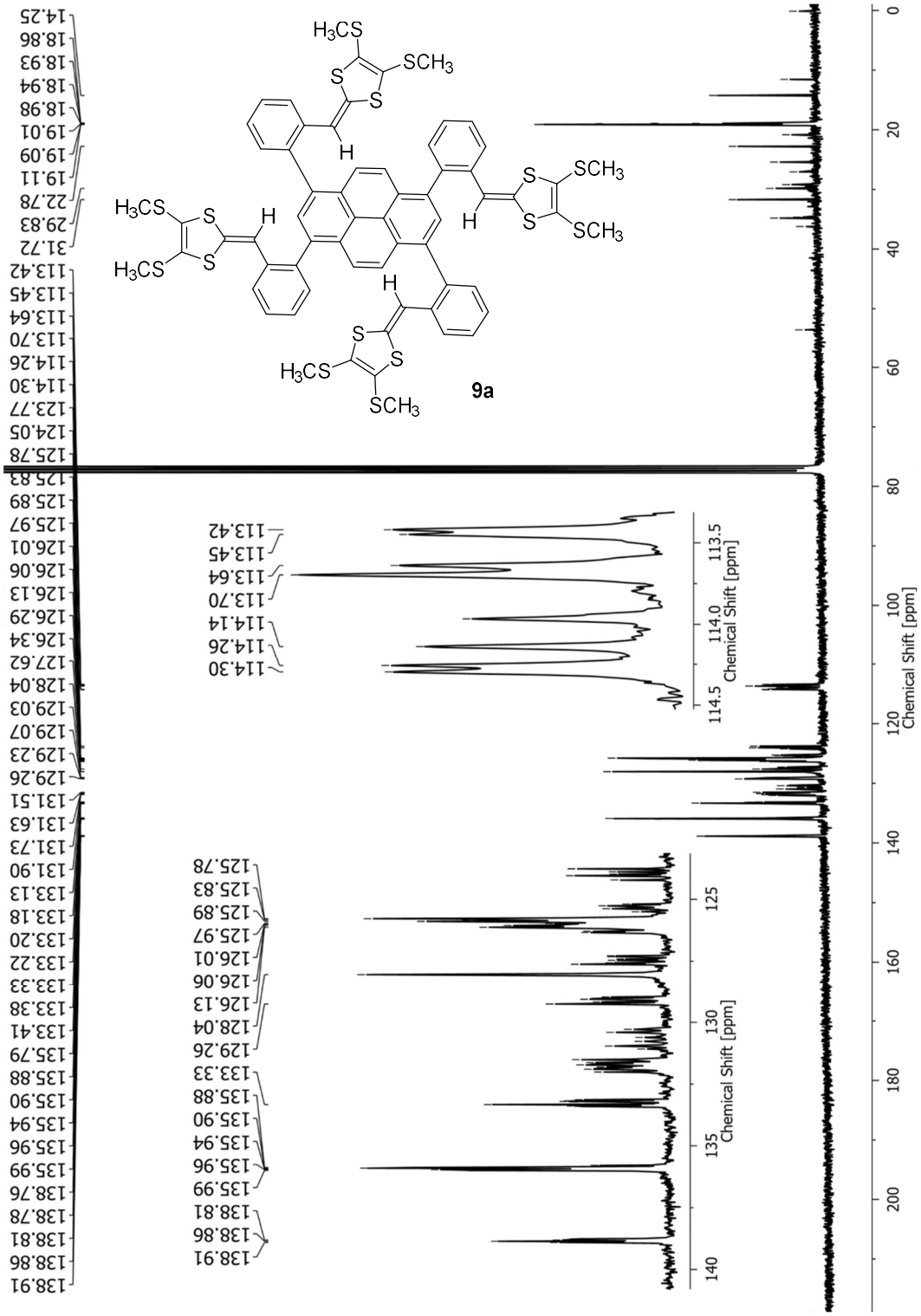

Fig. S-15 $^{13}C\{^{1}H\}$ NMR (75 MHz, $CDCl_3$) of compound **9a**.

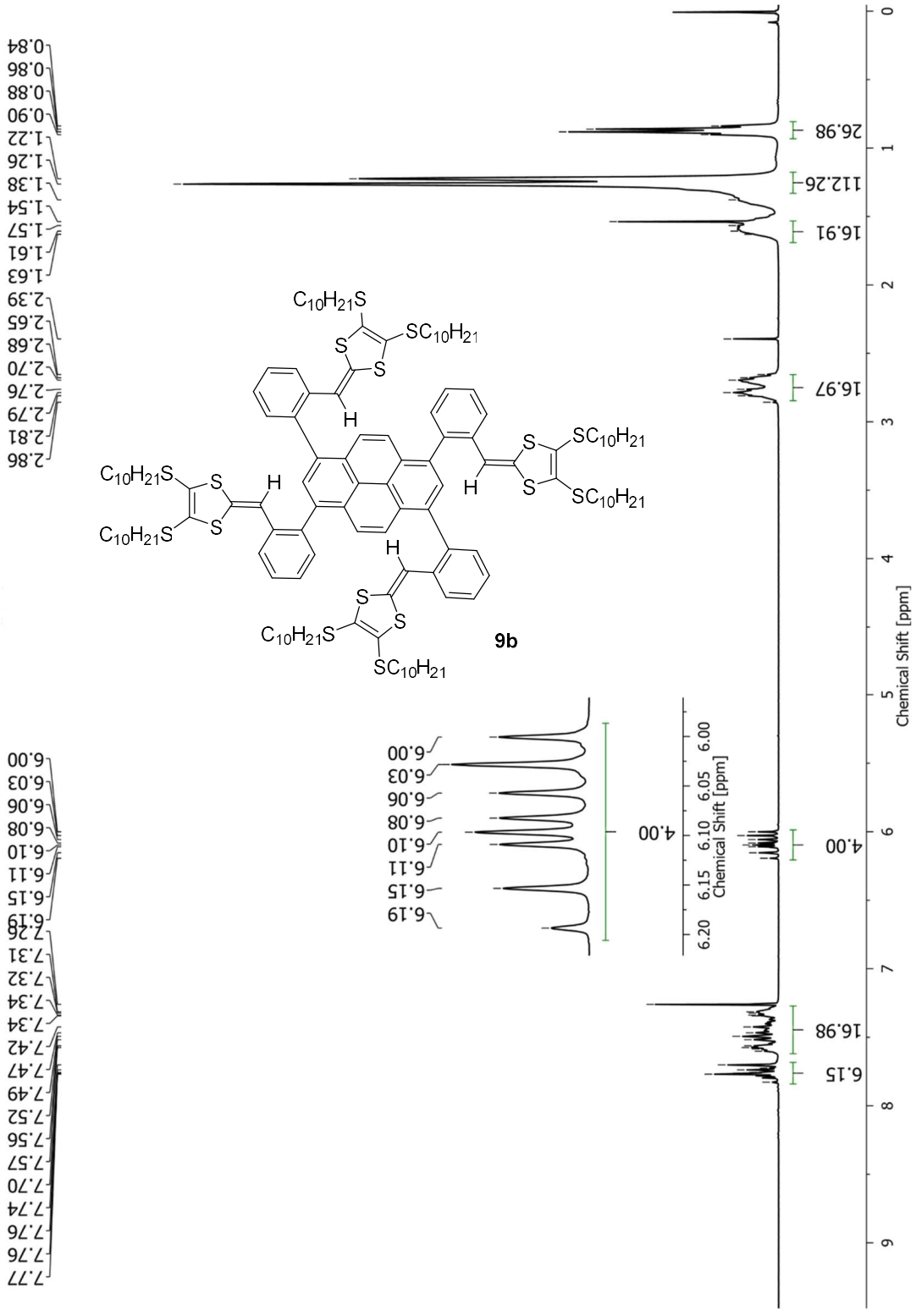

Fig. S-16 ^{1}H NMR (300 MHz, $CDCl_3$) of compound **9b**.

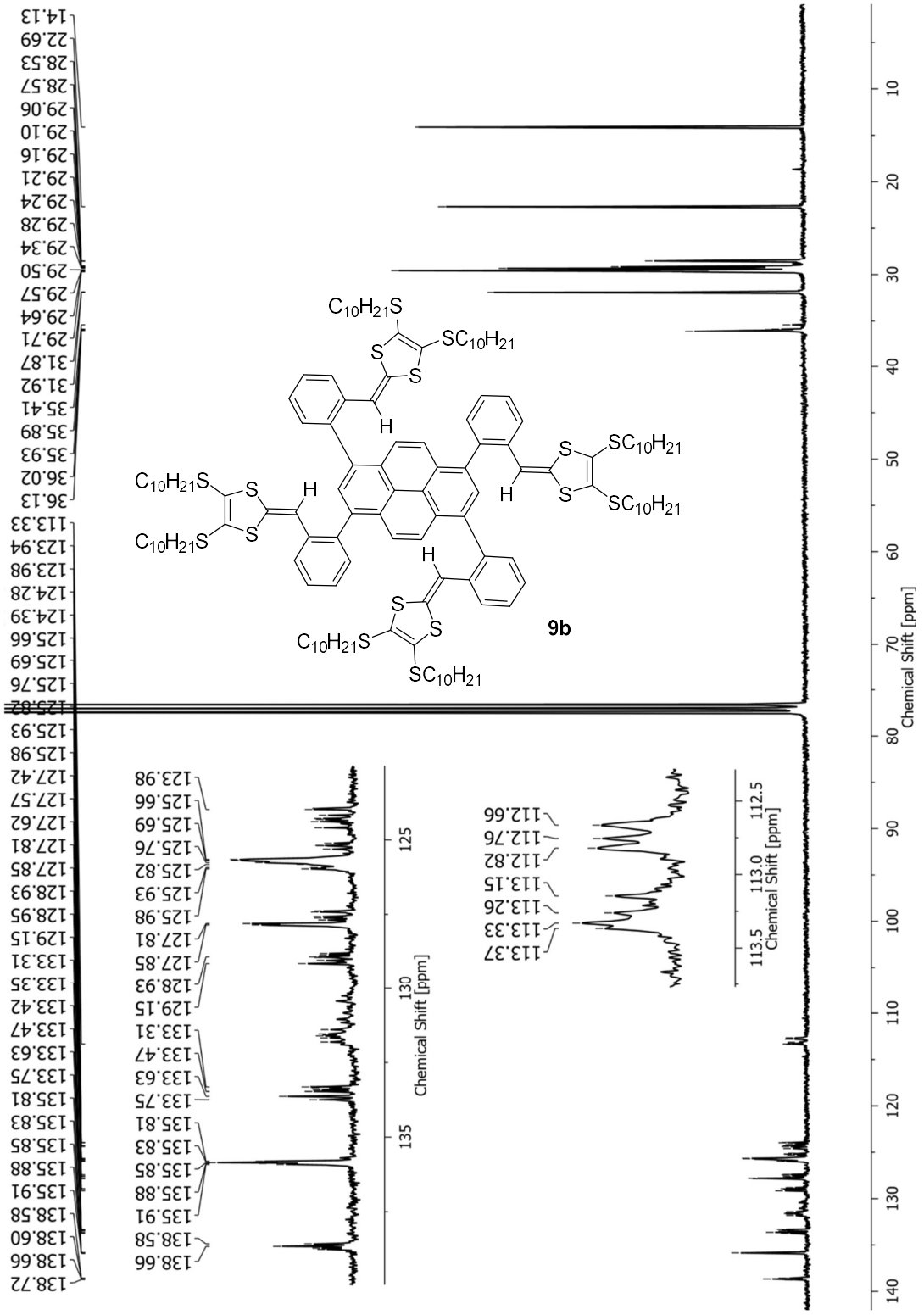

Fig. S-17 $^{13}C\{^{1}H\}$ NMR (75 MHz, $CDCl_3$) of compound **9b**.

2. Protonation/Deuterium Exchange Studies

Each sample of DTF-TPPys **7-9** (0.006 mmol) was dissolved with 0.60 mL of $CDCl_3$. To each of the solutions, TFA (0.01 mL, 0.130 mmol) was added and the mixture was shaken for 30 seconds (a dramatic color change from yellow to dark red was observed). After the TFA treatment, 0.60 mL of D_2O was added and the resulting mixture was neutralized with excess $NaHCO_3$. At last, the organic layer was separated, dried over $CaCl_2$, and filtered to yield corresponding deuterated DTF-TPPy. The proton/deuterium exchange efficiencies of all compounds were assessed based on ^1H NMR analysis using the following equations,

$$\left(\frac{I_V}{I_{Ar}}\right)_{before} = R_1 \qquad \left(\frac{I_V}{I_{Ar}}\right)_{after} = R_2$$

Where I_v is the integral of the vinylic proton of DTF group, and I_{Ar} refers to total integral of all aromatic (pyrenyl and phenyl) proton signals. Proton/deuterium exchange efficiency is calculated using the following equation.

$$\text{Proton/Deuterium Exchange Efficiency} = \left(\frac{R_1 - R_2}{R}\right) \times 100\%$$

In order to examine the reversibility of the DTF proton/deuterium exchange reactions, the deuterated samples in $CDCl_3$ were subsequently subjected to TFA treatment, quenched with H_2O instead of D_2O. The resulting solutions were then neutralized with $NaHCO_3$, and the organic layers were separated, dried over $CaCl_2$, and examined by ^1H NMR. In all cases, the vinylic proton signals were found to be fully recovered based on their relative integrals in the ^1H NMR spectra.

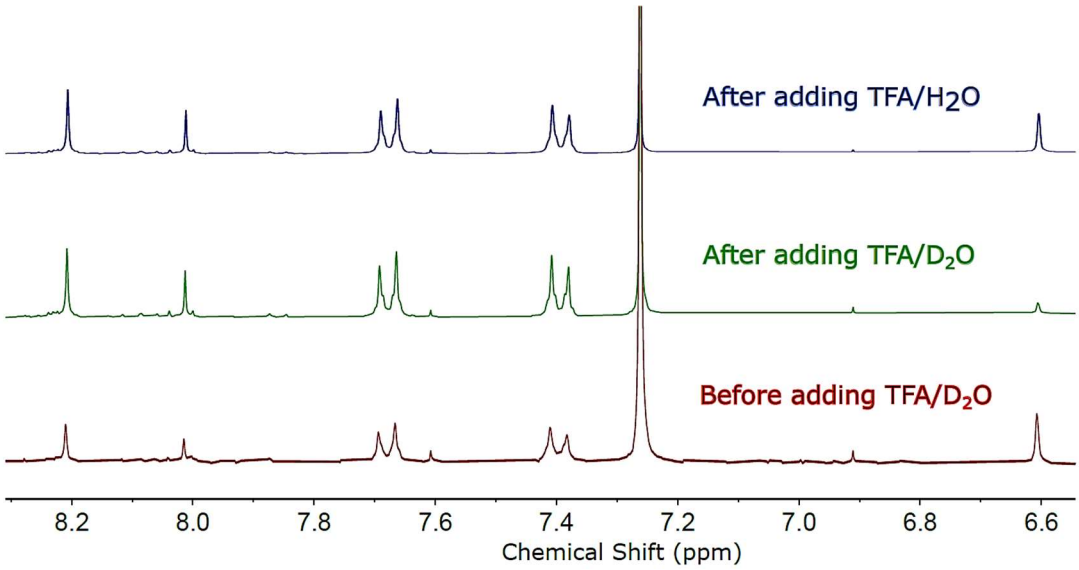

Fig. S-18 Expanded ^1H NMR spectra (300 MHz, $CDCl_3$) of **7a** before and after treatments of TFA/D_2O, and then TFA/H_2O.

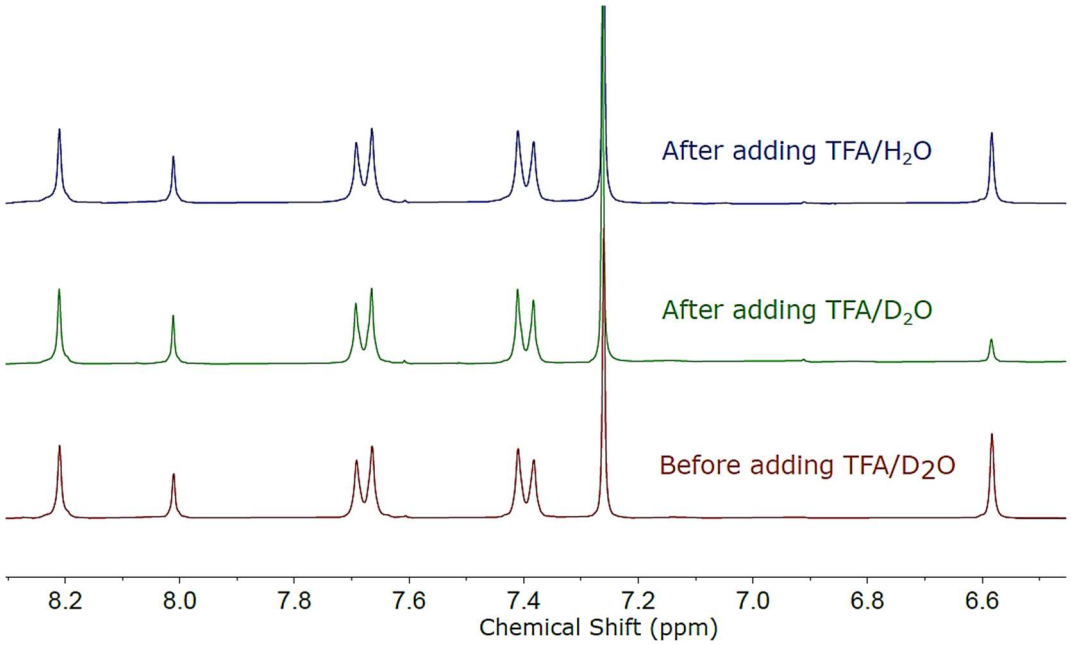

Fig. S-19 Expanded ^{1}H NMR spectra (300 MHz, $CDCl_3$) of **7b** before and after treatments of TFA/D_2O, and then TFA/H_2O.

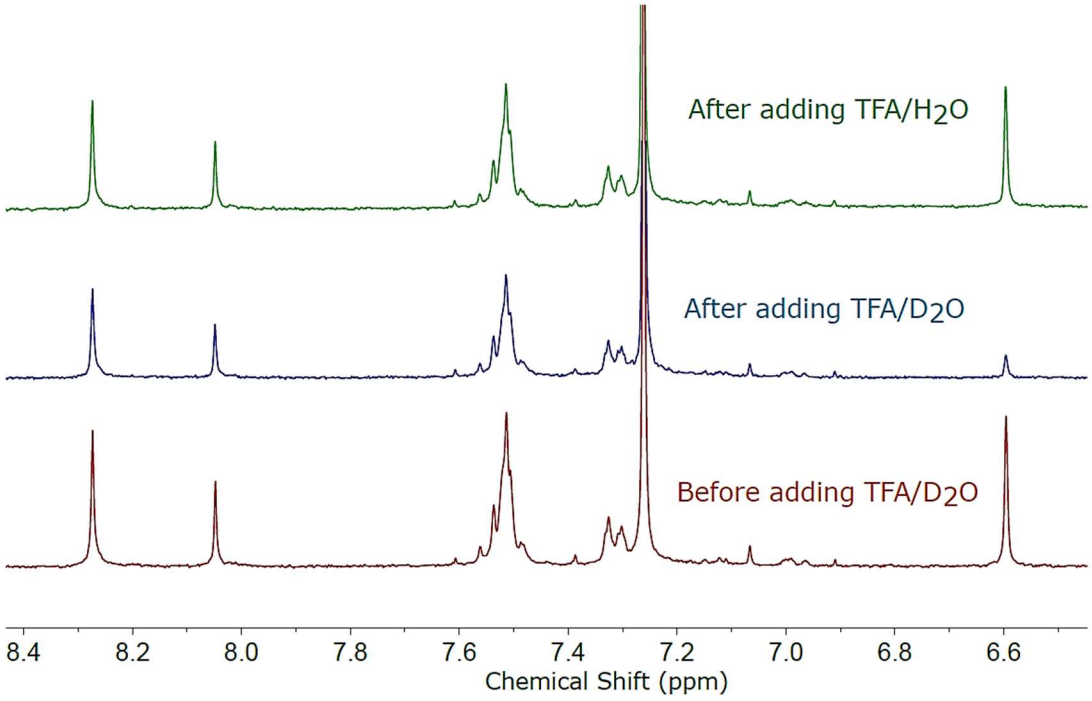

Fig. S-20 Expanded ^{1}H NMR spectra (300 MHz, $CDCl_3$) of **8a** before and after treatments of TFA/D_2O, and then TFA/H_2O.

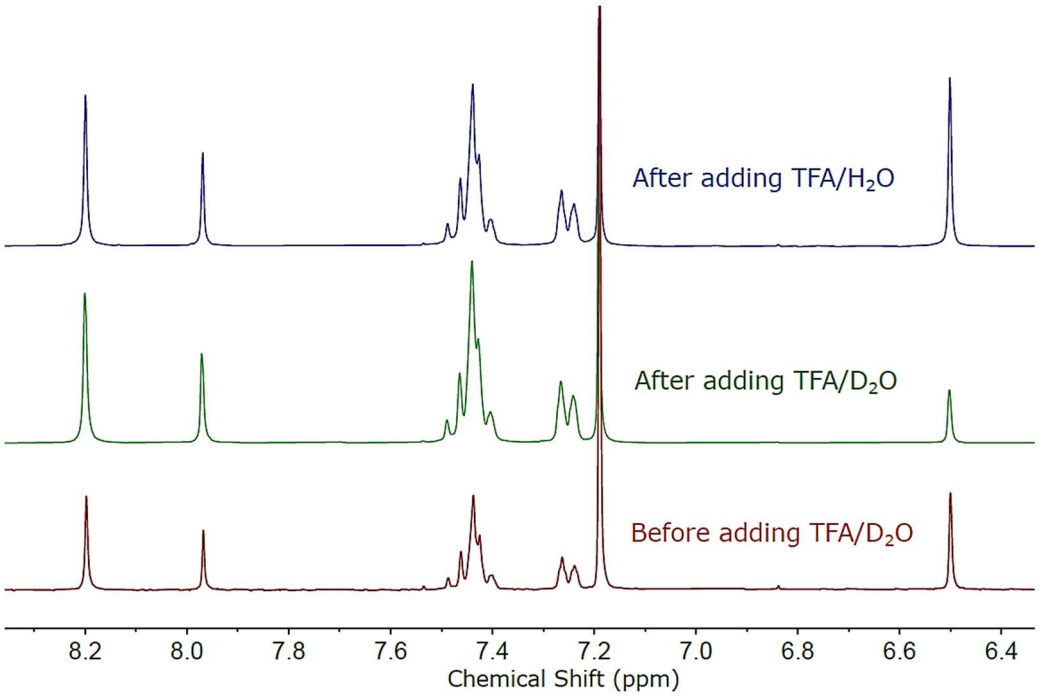

Fig. S-21 Expanded ^{1}H NMR spectra (300 MHz, $CDCl_3$) of **8b** before and after treatments of TFA/D_2O, and then TFA/H_2O.

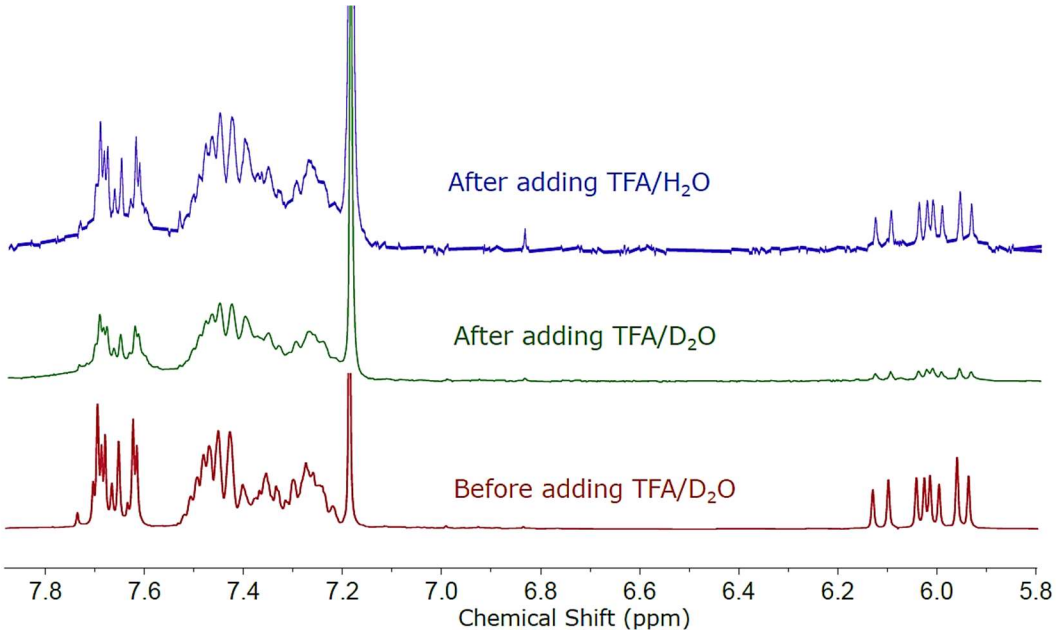

Fig. S-22 Expanded ^{1}H NMR spectra (300 MHz, $CDCl_3$) of **9a** before and after treatments of TFA/D_2O, and then TFA/H_2O.

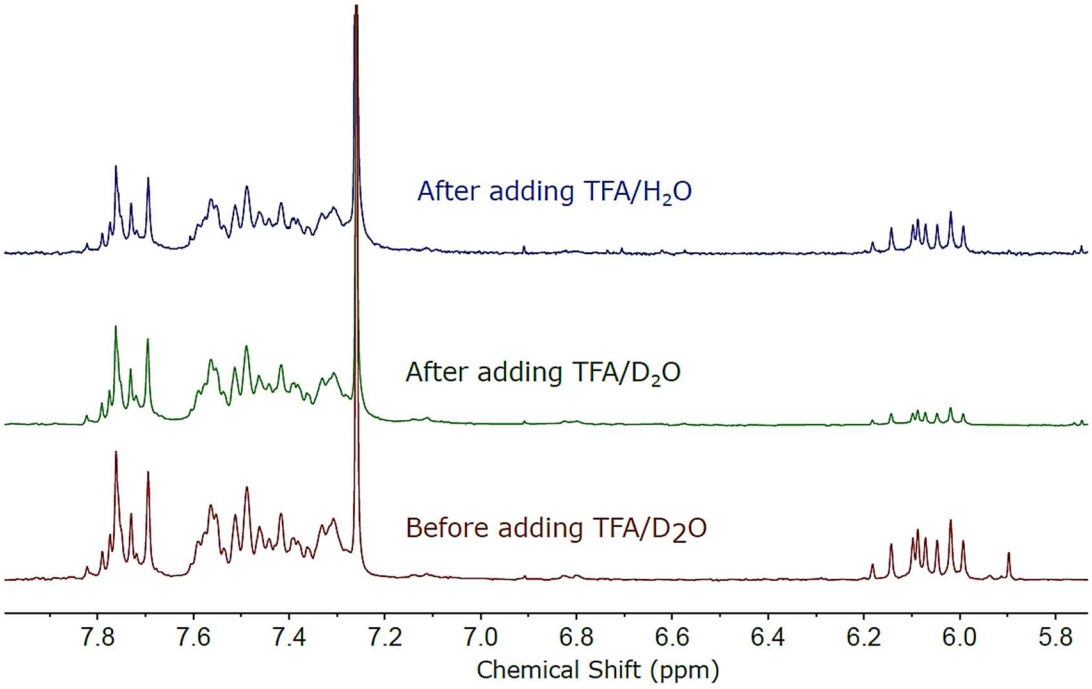

Fig. S-23 Expanded ^{1}H NMR spectra (300 MHz, $CDCl_3$) of **9b** before and after treatments of TFA/D_2O, and then TFA/H_2O.

3. UV-Vis Spectroscopic Data

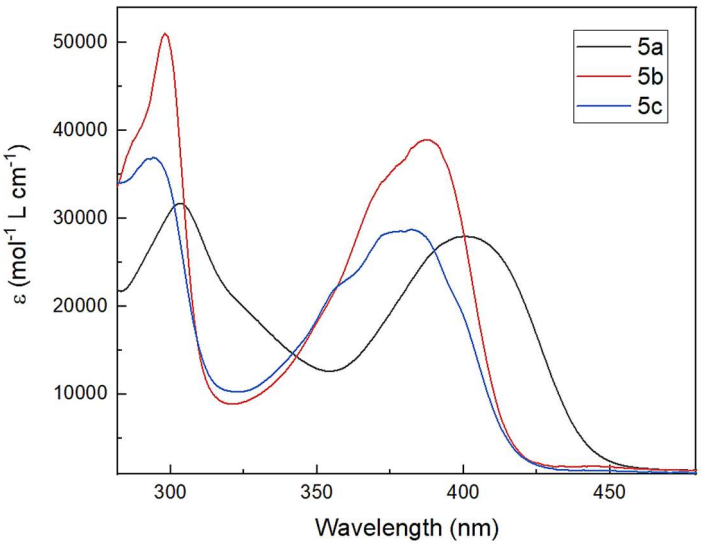

Fig. S-24 UV-Vis absorption spectra of compounds **5a**, 5**b**, and 5**c** measured in CH_2Cl_2.

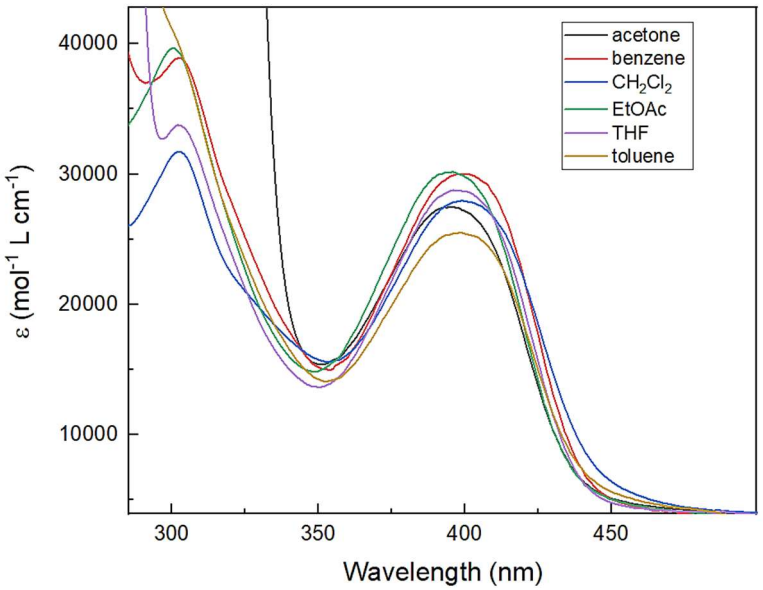

Fig. S-25 UV-Vis absorption spectra of **5a** measured in various organic solvents.

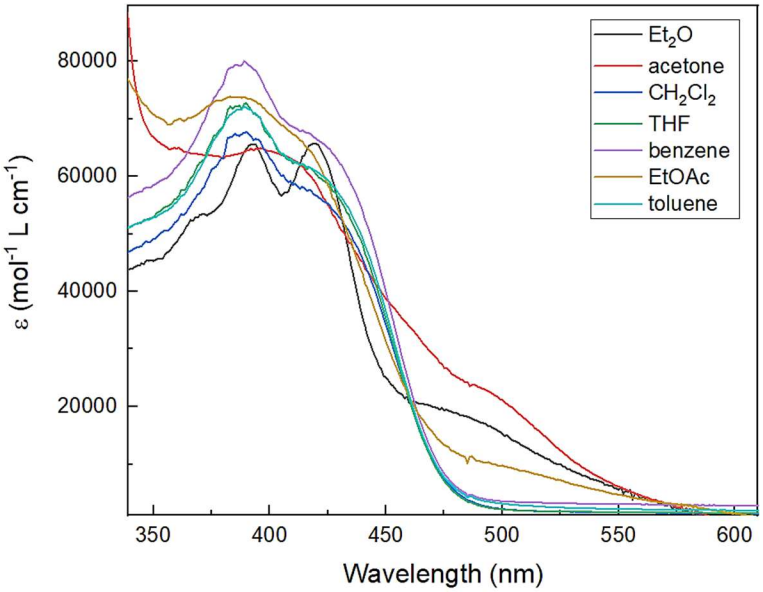

Fig. S-26 UV-Vis absorption spectra of **7a** measured in various organic solvents.

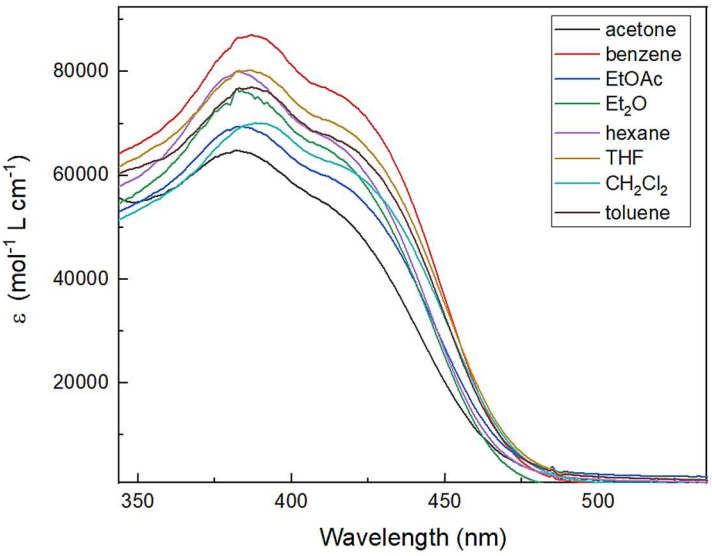

Fig. S-27 UV-Vis absorption spectra of **7b** measured in various organic solvents.

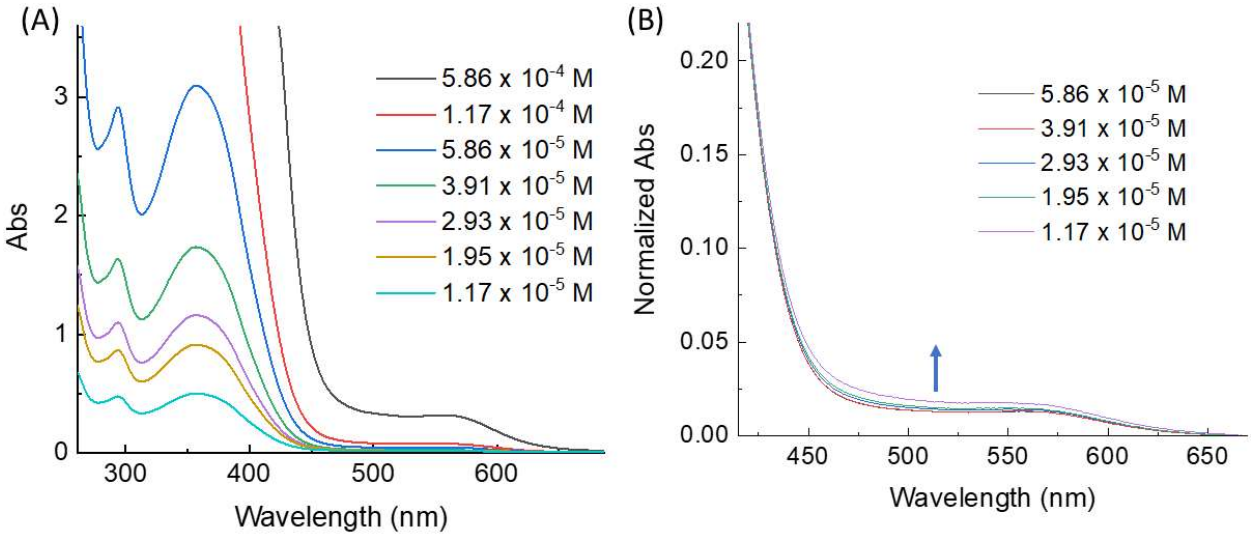

Fig. S-28 (A) UV-Vis absorption spectra of **9a** measured in CH_2Cl_2 at various concentrations. (B) Normalized UV-Vis absorption spectra of **9a** measured at various concentrations. The arrow indicates the increasing trend of absorption tail from 450 to 650 nm with increasing concentration.

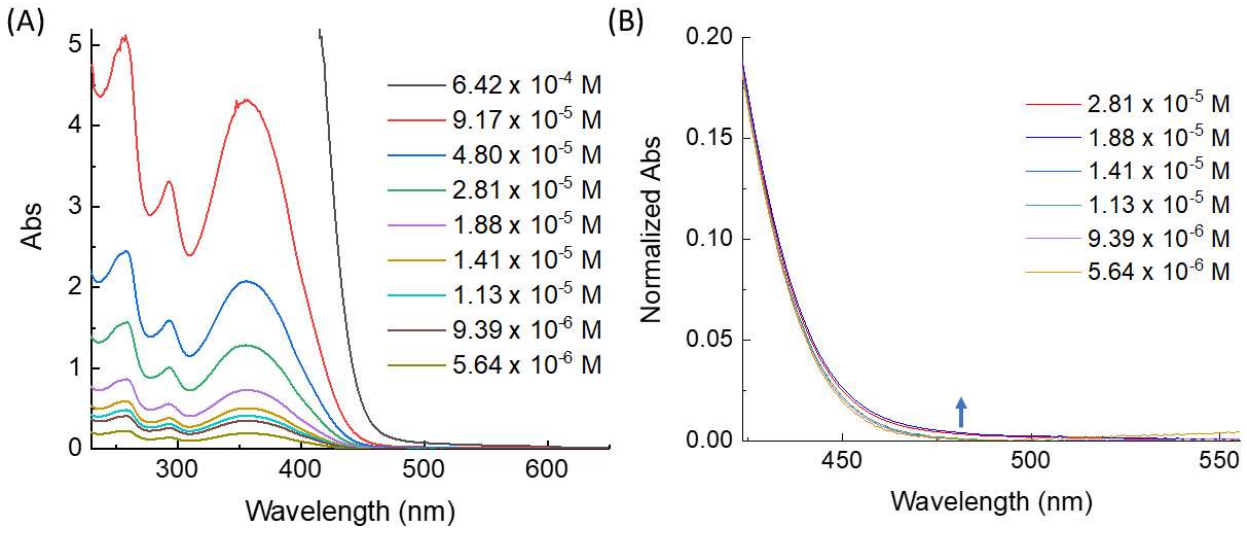

Fig. S-29 (A) UV-Vis absorption spectra of **9b** measured in CH_2Cl_2 at various concentrations. (B) Normalized UV-Vis absorption spectra of **9b** measured at various concentrations. The arrow indicates the increasing trend of absorption tail from 450 to 650 nm with increasing concentration.

4. Fluorescence Spectroscopic Data

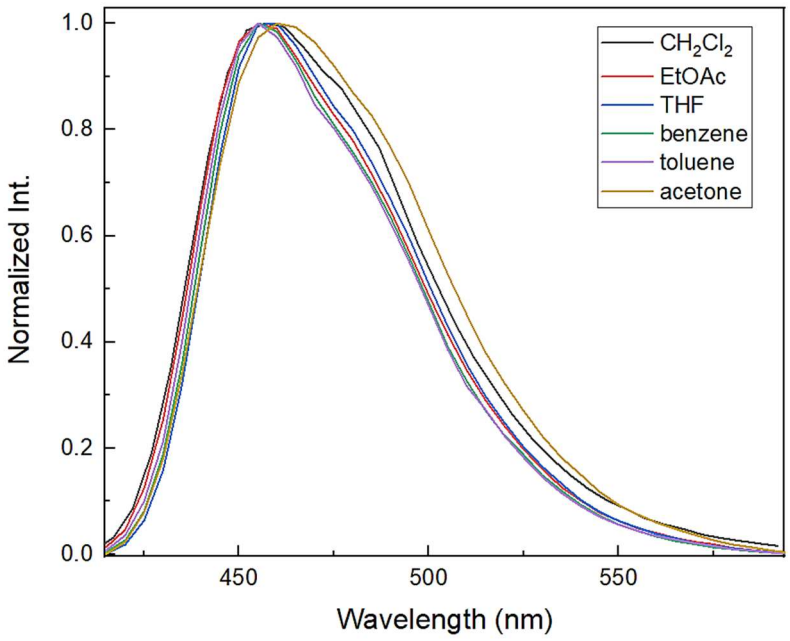

Fig. S-30 Normalized fluorescence spectra of **5a** measured in various organic solvents.

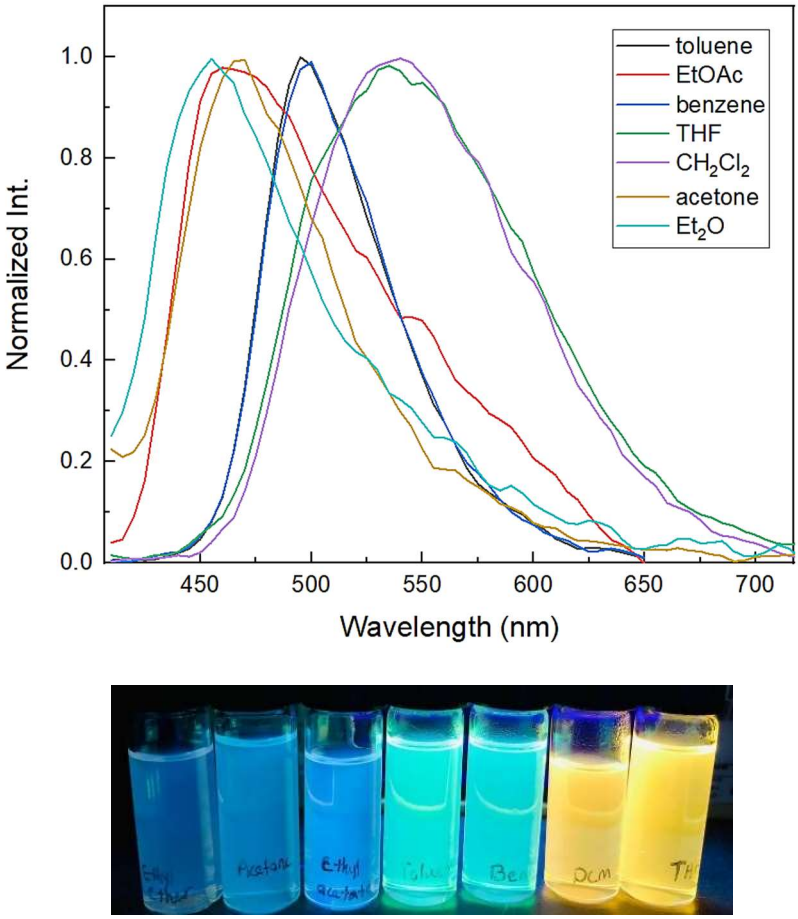

Fig. S-31 Normalized fluorescence spectra of **7a** measured in various organic solvents (top). Photographic image of the solutions of **7a** in various solvents under UV light (bottom). Solvents (from left to right): Et_2O, acetone, EtOAc, toluene, benzene, CH_2Cl_2, THF.

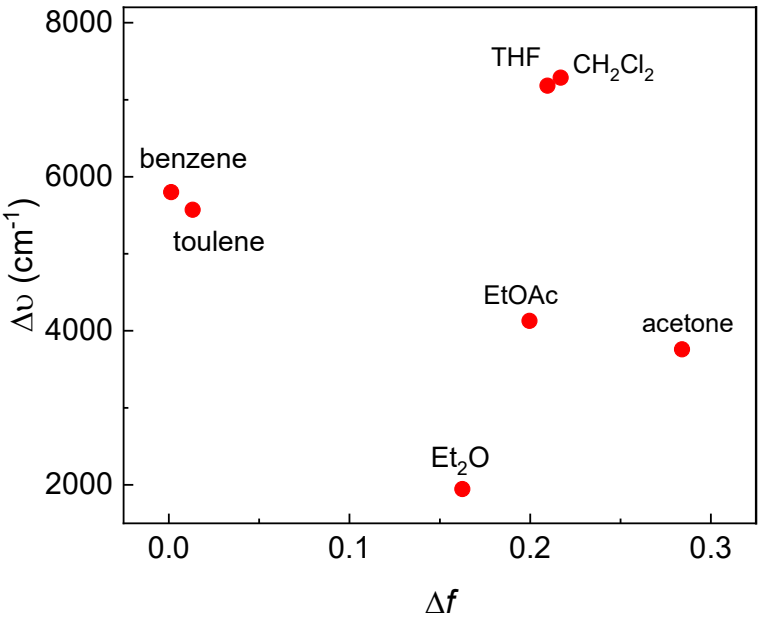

Fig. S-32 Correlation of observed Stokes shift ($\Delta\upsilon$) of **7a** and solvent orientation polarizability (Δf).

Table S-01 Summary of UV-Vis absorption and fluorescence data of compounds **5a**, **b**, and **c** measured in CH_2Cl_2

Compound	**UV-Vis absorption** λ_{max}**/nm (ε/mol^{-1} L cm^{-1})**	**Fluorescence** λ_{em}**/nm**
5a	401 (2.79×10^4), 303 (3.17×10^4)	465
5b	387 (3.90×10^4), 298 (5.09×10^4)	429
5c	380 (2.88×10^4), 294 (3.69×10^4)	435

Table S-02 Summary of UV-Vis absorption and fluorescence data of compounds **5a** in various organic solvents

Solvent	**UV-Vis absorption** λ_{max}**/nm (ε/mol^{-1} L cm^{-1})**	**Fluorescence** λ_{em}**/nm**
acetone	395 (2.75×10^4)	460
benzene	399 (3.00×10^4), 302 (3.89×10^4)	455
CH_2Cl_2	400 (2.79×10^4), 302 (3.18×10^4)	456
EtOAc	395 (3.02×10^4), 300 (3.98×10^4)	455
THF	398 (2.87×10^4), 303 (3.38×10^4)	457
toluene	399 (2.55×10^4), Sh 303 (3.98×10^4)	455

Table S-03 Summary of UV-Vis absorption and fluorescence data of compounds **7a** in various organic solvents

Solvent	**UV-Vis absorption** λ_{max}**/nm (ε/mol^{-1} L cm^{-1})**	**Fluorescence** λ_{em}**/(nm)**
Et_2O	488 (sh, 1.75×10^4), 418 (6.60×10^4), 392 (6.56×10^4)	455
acetone	498 (sh, 2.17×10^4), 398 (6.44×10^4)	468
CH_2Cl_2	420 (sh, 5.65×10^4), 387 (6.76×10^4)	539
THF	420 (sh, 6.05×10^4), 387 (7.23×10^4)	536
benzene	422 (sh, 6.61×10^4), 387 (7.94×10^4)	499
EtOAc	416 (sh, 6.50×10^4), 388 (7.39×10^4)	462
toluene	421 (sh, 6.04×10^4), 388 (7.18×10^4)	495

Table S-04 Summary of UV-Vis absorption and fluorescence data of compounds **7b** in various organic solvents

Solvent	**UV-Vis absorption** λ_{max}**/nm (ε/mol^{-1} L cm^{-1})**	**Fluorescence** λ_{em}**/(nm)**
acetone	416 (sh, 5.24×10^4), 382 (6.49×10^4)	572
benzene	419 (sh, 7.42×10^4), 387 (8.71×10^4)	498
EtOAc	419 (sh, 5.74×10^4), 382 (6.90×10^4)	514
Et_2O	414 (sh, 6.39×10^4), 383 (7.64×10^4)	495
hexane	418 (sh, 6.44×10^4), 382 (7.99×10^4)	487
THF	419 (sh, 6.84×10^4), 386 (8.02×10^4)	523
CH_2Cl_2	420 (sh, 6.05×10^4), 388 (7.00×10^4)	538
toluene	419 (sh, 6.47×10^4), 387 (7.67×10^4)	495

5. X-ray Single Crystallographic Data of 5c and 10

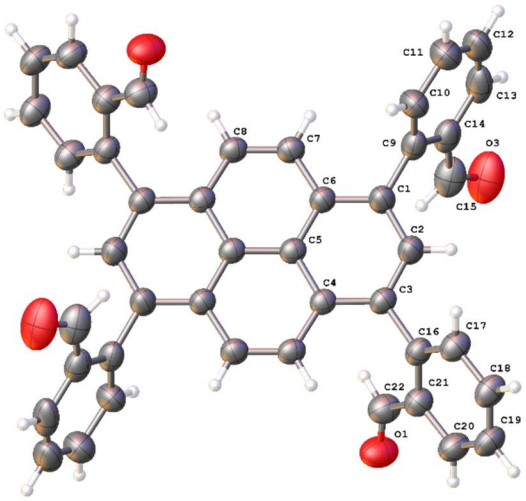

Fig. S-33 X-ray crystal structure of **5c** (non-hydrogen atoms are represented by displacement ellipsoids at the 50% probability level).

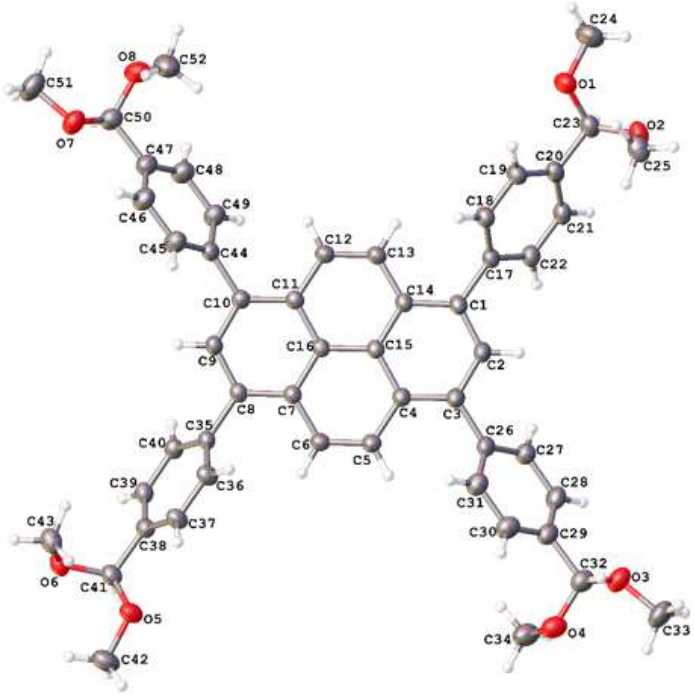

Fig. S-34 X-ray crystal structure of **10** (non-hydrogen atoms are represented by displacement ellipsoids at the 50% probability level).

Table S-05 Crystal data and structure refinement of **5c**

Empirical formula	C50H38O4
Formula weight	702.80
Temperature/K	100(2)
Crystal system	monoclinic
Space group	P21/c
a/Å	11.1936(2)
b/Å	21.2734(3)
c/Å	7.72170(10)
β/°	109.217(2)
Volume/Å3	1736.28(5)
Z	2
ρcalcg/cm3	1.344
μ/mm-1	0.661
F(000)	740.0
Crystal size/mm3	0.311 × 0.172 × 0.161
Radiation	Cu Kα (λ = 1.54184)
2θ range for data collection/°	8.312 to 154.568
Index ranges	-13 ≤ h ≤ 14, -26 ≤ k ≤ 25, -9 ≤ l ≤ 9
Reflections collected	18375
Independent reflections	3637 [Rint = 0.0374, Rsigma = 0.0277]
Data/restraints/parameters	3637/14/324
Goodness-of-fit on F2	1.100
Final R indexes [I>=2σ (I)]	R1 = 0.0878, wR2 = 0.2557
Final R indexes [all data]	R1 = 0.0908, wR2 = 0.2582
Largest diff. peak/hole / e Å-3	0.43/-0.52

Table S-06 Crystal data and structure refinement of **10**

Empirical formula	$C_{52}H_{50}O_8$
Formula weight	802.92
Temperature/K	100(2)
Crystal system	orthorhombic
Space group	*Pbcn*
a/Å	15.66880(10)
b/Å	9.35570(10)
c/Å	56.7594(5)
Volume/Å^3	8320.51(13)
Z	8
ρ_{calc}g/cm^3	1.282
μ/mm^{-1}	0.686
F(000)	3408.0
Crystal size/mm^3	0.095 × 0.079 × 0.056
Radiation	Cu *K*α (λ = 1.54184)
2θ range for data collection/°	6.228 to 154.818
Index ranges	$-13 \le h \le 19$, $-11 \le k \le 11$, $-71 \le l \le 69$
Reflections collected	56336
Independent reflections	8698 [R_{int} = 0.0445, R_{sigma} = 0.0326]
Data/restraints/parameters	8698/0/549
Goodness-of-fit on F^2	1.037
Final *R* indexes [I>=2σ (I)]	R_1 = 0.0570, wR_2 = 0.1608
Final *R* indexes [all data]	R_1 = 0.0691, wR_2 = 0.1716
Largest diff. peak/hole / e Å^{-3}	0.48/-0.25

6. Rotational Properties of Compound 5c

The rotational properties of compound **5c** were investigated by variable-temperature (VT) NMR analysis in conjunction with *ab initio* modeling. VT NMR analysis was performed on a Bruker AVANCE 500 spectrometer equipped with a TXI inverse triple resonance probe.

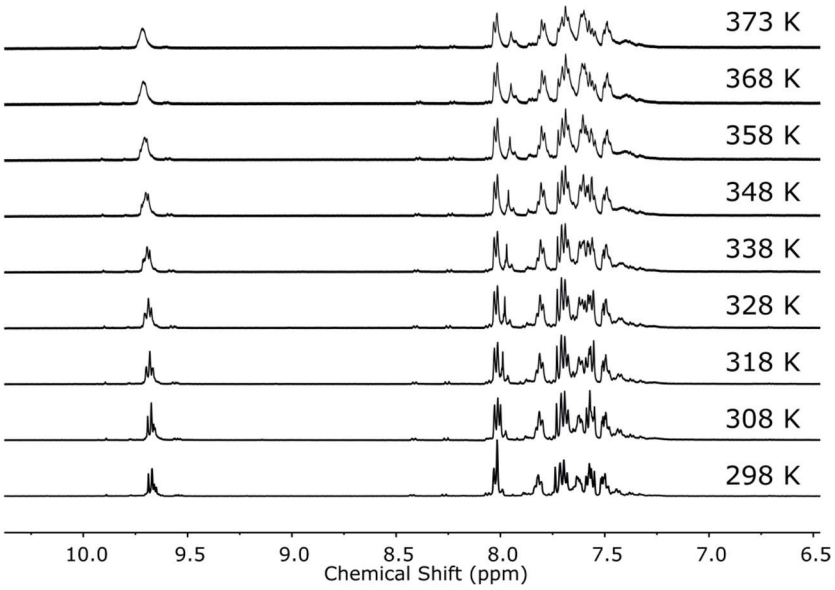

Fig. S-35 VT ^{1}H NMR spectra (500 MHz, DMSO-d_6) of **5c** showing the region of aldehyde and aromatic proton signals measured at different temperatures.

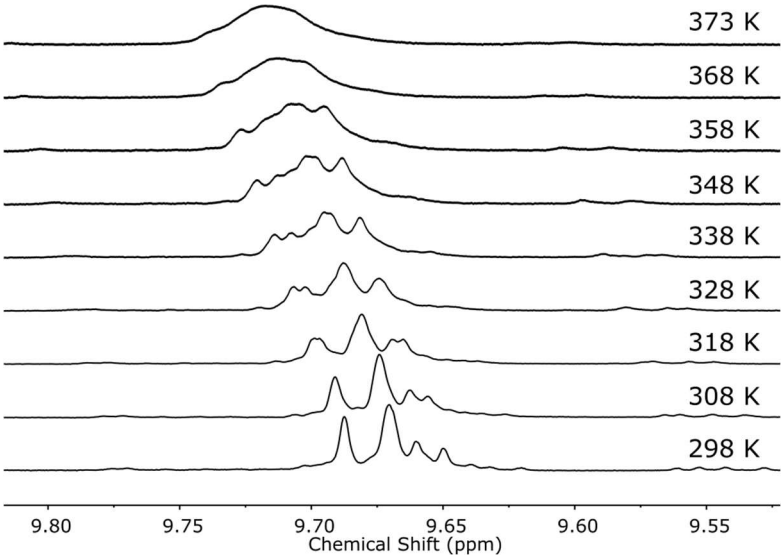

Fig. S-36 VT ^{1}H NMR spectra (500 MHz, DMSO-d_6) of **5c** showing the region of aldehyde proton signals measured at different temperatures.

To further assess the rotational energy barriers in the structure of **5c**, a model compound **11** was modeled at the B3LYP-D3/6-31G(d) level using the *Spartan'18* software package (Wavefunction Inc., Irvine, CA, USA). Our computational results disclose two rotational transition states (namely **TS-1** and **TS-2**). As shown in Scheme S-1, the **TS-1** has a lower rel. *G* (22.77 kcal/mol) than **TS-2** (30.64 kcal/mol). The interconversion among the atropisomers of **5c** will require to overcome an energy barrier of at least 22.77 kcal/mol.

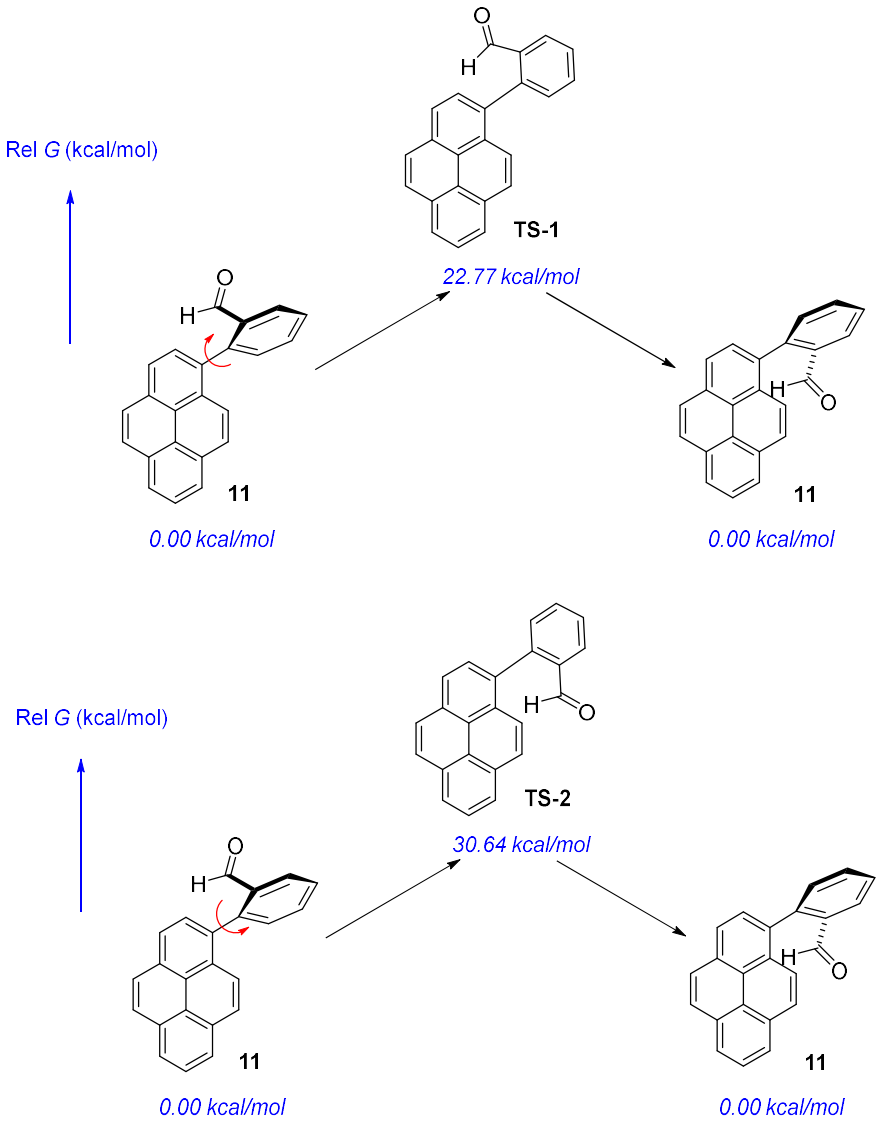

Scheme S-01 Two rotational transition states for model compound **11** and their relative Gibbs free energies (in kcal/mol).

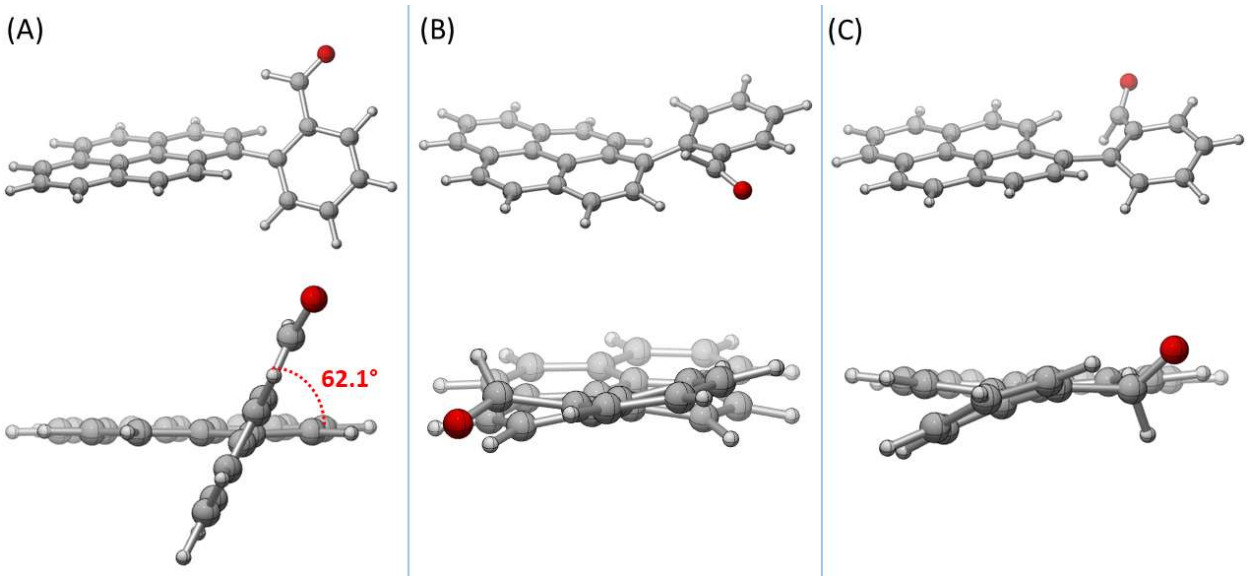

Fig. S-37 Optimized geometries of model compound **11** (A) in the ground state, (B) rotational transition state **TS-1**, and (C) rotational transition state **TS-2**. Calculations performed at the B3LYP-D3/6-31G(d) level of theory.

Cartesian coordinates of optimized geometry of **11** (*E* = -960.185093 Hartree, *G* = -959.934043 Hartree, dipole moment = 3.65 Debye)

H	-0.424333	0.799271	-3.196802
C	-0.333994	0.914550	-2.120140
C	-0.159423	1.200720	0.662475
C	-0.119154	-0.228442	-1.336944
C	-0.467128	2.174441	-1.550433
C	-0.397932	2.343101	-0.160047
C	-0.008014	-0.093084	0.069443
H	-0.644199	3.039271	-2.184650
C	-0.081010	1.354737	2.078906
C	0.052017	1.651844	4.871044
C	0.170414	0.221585	2.909552
C	-0.259031	2.642073	2.671098
C	-0.190392	2.764839	4.067492
C	0.233543	0.393483	4.300981
H	-0.329150	3.744247	4.518160
H	0.425082	-0.471335	4.931371
H	0.101530	1.766687	5.950181
C	-0.566091	3.625658	0.461304

H	-0.749623	4.485864	-0.177801
C	-0.503610	3.768275	1.813182
H	-0.637502	4.745850	2.269165
C	0.274442	-1.207852	0.933923
H	0.431822	-2.184690	0.489305
C	0.357767	-1.056538	2.284086
H	0.575175	-1.915208	2.914910
C	-0.099315	-1.565478	-2.002457
C	-0.247161	-4.065184	-3.317618
C	0.849803	-1.922684	-2.986922
C	-1.108469	-2.492409	-1.690896
C	-1.183211	-3.725176	-2.335139
C	0.760329	-3.164976	-3.636949
H	-1.852042	-2.226292	-0.945391
H	-1.979095	-4.418806	-2.076487
H	1.511942	-3.398683	-4.384816
H	-0.306638	-5.024938	-3.823301
C	1.998215	-1.045761	-3.332927
H	2.124148	-0.146699	-2.699777
O	2.780286	-1.282264	-4.237080

Cartesian coordinates of optimized geometry of **TS-1** (E = -960.152583 Hartree, G = -959.897750 Hartree, dipole moment = 3.91 Debye, imaginary frequency = i31 cm^{-1})

H	0.410908	0.797889	-3.102001
C	0.244657	0.863978	-2.034902
C	0.128205	1.173953	0.724554
C	0.205495	-0.314633	-1.256563
C	0.096693	2.131626	-1.499053
C	-0.068947	2.307060	-0.120077
C	0.360617	-0.126456	0.160525
H	0.089447	2.996258	-2.157875
C	0.103127	1.359682	2.141855
C	-0.011535	1.703180	4.934359
C	0.417544	0.278195	3.015349
C	-0.230034	2.634166	2.695486
C	-0.296593	2.775635	4.090395
C	0.355908	0.468843	4.404740
H	-0.569571	3.741294	4.509163
H	0.601239	-0.360860	5.063389
H	-0.066346	1.834663	6.011591
C	-0.372170	3.581903	0.458074
H	-0.530227	4.424328	-0.211135
C	-0.474405	3.734656	1.806472

H	-0.725286	4.701723	2.235294
C	0.830840	-1.136650	1.073424
H	1.265018	-2.043612	0.674981
C	0.852364	-0.949352	2.422913
H	1.239400	-1.732989	3.070376
C	-0.012585	-1.628664	-1.927755
C	-0.107953	-4.194394	-3.208572
C	-0.171735	-1.758459	-3.346407
C	-0.121478	-2.838952	-1.205469
C	-0.160640	-4.087530	-1.819976
C	-0.148325	-3.023426	-3.955515
H	-0.212474	-2.816602	-0.130633
H	-0.235317	-4.978397	-1.201180
H	-0.230787	-3.058184	-5.038000
H	-0.103751	-5.164561	-3.697485
C	-0.631759	-0.685161	-4.277175
H	-1.382360	0.008893	-3.846084
O	-0.337183	-0.619042	-5.457083

Cartesian coordinates of optimized geometry of **Ts-2** (*E* = -960.139042 Hartree, *G* = -959.885215 Hartree, dipole moment = 3.16 Debye, imaginary frequency = i69 cm^{-1})

H	-1.163439	0.447207	-3.055558
C	-0.810154	0.671224	-2.058661
C	-0.180675	1.306552	0.567273
C	-0.207476	-0.356946	-1.292032
C	-1.015585	1.959845	-1.605970
C	-0.661998	2.326161	-0.304700
C	0.009772	-0.044239	0.092511
H	-1.468045	2.694315	-2.267519
C	0.084032	1.653925	1.931721
C	0.584899	2.328045	4.626728
C	0.499169	0.660049	2.864385
C	-0.089619	2.999419	2.385222
C	0.171083	3.310182	3.729056
C	0.745435	1.012835	4.200680
H	0.036850	4.334935	4.066251
H	1.054420	0.241223	4.901394
H	0.774563	2.588785	5.664084
C	-0.824286	3.668069	0.168944
H	-1.184928	4.417579	-0.531138
C	-0.542741	3.995518	1.458003
H	-0.670246	5.015375	1.811905
C	0.354834	-1.006546	1.097223
H	0.354410	-2.049121	0.845267

C	0.590826	-0.686861	2.398559
H	0.823688	-1.474318	3.111076
C	0.071578	-1.625006	-2.082076
C	-0.121481	-3.785671	-3.980865
C	0.113369	-2.997354	-1.669841
C	0.167955	-1.446111	-3.486635
C	0.077065	-2.479303	-4.414454
C	-0.063767	-4.026550	-2.614367
H	0.319854	-0.448859	-3.878314
H	0.151223	-2.251031	-5.474276
H	-0.095285	-5.043744	-2.236761
H	-0.253178	-4.604100	-4.682543
C	0.621074	-3.585397	-0.391035
H	1.584372	-3.151598	-0.051502
O	0.162435	-4.568487	0.157966